Original Article

New Molecular Imprinting Nano Polymer Synthesis And Characterization As A Biocompatible For Drug Delivery Applications

Hayfaa Jasim Mohammed[1]*, Mohammed Ali Mutar[2]

*[1]Department of Chemistry / Faculty of Education for Girls/Kufa University/Iraq-Najaf, hayfaa.sinbah@uokufa.edu.iq
[2]Department of Chemistry / Faculty of Science / University of AL-Qadisiyah, IRAQ, mohammed.ali@qu.edu.iq

***Corresponding Author:-** Hayfaa Jasim Mohammed
Department of Chemistry / Faculty of Education for Girls/Kufa University/Iraq-Najaf, hayfaa.sinbah@uokufa.edu.iq
Doi: 10.47750/pnr.2022.13.S05.27

Abstract

New polymeric nanoparticles were to be developed for biomedical purposes as the purpose of this study. It was thought that the production of materials with novel properties and functions could be accomplished by meticulous design and synthesis, as well as the research of structure-property connections. A novel method that we developed has excellent sensitivity, cheap cost, and high stability. The molecularly imprinted polymer (MIP) used in this method, which is based on a functional monomer named polylactic acid (PLA), Acrylic acid (AA) , Methylacrylate (MA) Chitosan (Cs), Bisphenol A dimethacrylate(BADMA) , N,N-dimethylacrylamide(DMA), Polyvinylpyrrolidone (PVP), Ethylene glycol(EG), Methyl Methacrylate(MMA). To search into the potential use of these hydrogels in controlled drug delivery systems, were crosslinked by 1,6 hexanedioldiacrylate (HDODA) and photoinitiated by 1-hydroxycyclohexyl phenyl ketone before being polymerized using free radical polymerization.

We synthesized the water-insoluble, amphiphilic polymer MIPs and for the first time described its structure and characteristics. This polymer, which has a nanostructure with a size of about 40-88 nm, is the ideal biocompatible polymer for nanobioapplications. Atenolol was loaded onto a produced hydrogel, and the drug release of such hydrogels in vitro and in vivo was studied. According to the results, raising the pH accelerated the rate of drug release. Fourier transform infrared and 1HNMR spectroscopy, thermal gravimetric measurement, and scanning electron microscopy were used to analyze the produced hydrogels. I have been studying about the TGA and DSC utilizing argon medium gas and a 10 oC/min heating rate. The effect of TGA shows% residue between 2-12% at 500ºC and char yield between 26- 50% at 400ºC. Nanocopolymer hydrogels' glass transition values (Tg) ranged from 120 to 275 °C.

The faculty of biological science and biotechnology at Shahid Beheshti University also conducted studies on the efficiency of these nanocopolymers using laboratory rats., Tehran, Iran on 18 Male Wistar rats weighing 200–240 g and divided rats into several groups, a group of natural control, and other groups for the induction of high pressure by Nacl (1%) and Dexamethasone, which includes a high pressure control group, , groups of treatment with polymers loaded with (Atenolol), and high pressure control groups, where The results showed that polymers have an obvious effect on lowering blood pressure levels in rats. Additionally, to avoid the issue of increased loading (Atenolol) caused by the treatment process (Atenolol), which is normally what happens as a result of an overdose, as well as to reduce the number of periodic blood pressure checks.

Keywords: Atenolol, Molecularly imprinted polymer, Nanocoploymers , Drug release, 1,6 hexanedioldiacrylate (HDODA), photo initiator, in vivo ,in vitro, thermo gravimetric analysis ,rats.

INTRODUCTION

Solid and colloidal macromolecular particles with a size less than 100 nm are known as nanoparticles[1,2]. The exploration of various nano compositions is a result of many application areas. For example, they can create metal-based NPs, polymeric NPs, biological NPs, and lipid-based NPs[3-6]. Polymeric nanoparticles are produced using biocompatible and biodegradable polymers. Polymers are used as biomaterials as a result of beneficial properties such like excellent biocompatibility, biodegradability, simplicity of synthesis and design, variety of chemical structures, and intriguing biological imitative character [7].

To overcome the drawbacks of classic medication formulations, controlled drug delivery systems—meant to administer pharmaceuticals have been developed at predetermined rates for predetermined lengths of time. If the active agents were delivered by a system that recognized the signal produced by sickness, it would be very beneficial, After evaluating the signal's strength, the required steps were taken to release the proper dosage of medication. A feedback mechanism would be necessary in such a system to connect the drug delivery rate to the physiological requirement [8]. The environmentally sensitive "smart" polymers are ideal candidates for developing self-regulating drug delivery systems. The pH change in the environment may be the most significant physiological stimulation. The pH-sensitive polymers have attached basic or acidic groups, such as ammonium salts or carboxylic and sulfonic acids , that, depending on

variations in the pH of the environment, either accept or release protons. Polyelectrolytes, which include polyanions and polycations, are polymers with many ionizable groups. Polyelectrolytes' pendant acidic or basic groups, like the acidic or basic groups of monoacids or monobases, are ionized. The most commonly used polymers in the development of enteric coated formulations for oral administration are pH sensitive ones. Since the intestines' neutral pH is significantly different from that of the stomach's pH (<3), the polyelectrolyte polymer will act differently depending on the pH . As a result, the drug's potency decreased If they are not shielded by orally administered products, which are designed to withstand the acidic juices of the stomach and then release the medication at the higher pH of the small intestine (above pH 5.5) or the much higher pH of the colon (above pH 6.5) [9].

A rapidly evolving technique for producing polymeric materials with high molecular recognition is molecular imprinting. By using radical polymerization, the functional monomers are typically cross-linked when the template molecules are present before the target molecules are eliminated. Selective rebinding between the template molecules and the imprinted polymers occurs [10]. The synthesis procedure is simple and inexpensive, and the polymers that are produced are reliable, adaptable, and good resistance to a wide range of pHs, solvents, and temperatures. Due to these characteristics, MIPs can be applied to a variety of templates, such as drugs, peptides, proteins, nucleotides, amino acid derivatives, and environmental contaminants [11]. Widespread interest is being shown in it, particularly in drug delivery, chemical sensors, chromatography, and solid-phase extraction (SPE) [12]. A suitable solvent is used to combine The MIP is synthesized using a functional monomer, a template, a cross-linker, and an initiator [13]. This method has several advantages, including the ability to produce simple template-monomer complexes, simple template removal from polymers, quick template binding to MIPs, and excellent application to a wide and varied set of target molecule. However, To produce the labile complex of template and monomer as efficiently as possible, To reduce non-specific binding sites, the polymerization conditions must be carefully controlled [14]. This study produced an efficient nano-MIP with potent drug identification and absorption capacities.

EXPERIMENTAL

Materials

1,6-hexanedioldiacrylate(HDODA)(ALDRICH), PolyLacticacid(PLA) ALDRICH, Acrylic acid(AA) HIMEDIA, Methylcellulose(MC) ALDRICH, 1-hydroxycyclohexyl phenyl ketone(photoinitiator) ALDRICH, nitrogen purged, Distilled water,phosphate buffer saline(PBS)HIMEDIA .

INSTRUMENTS

FTIR 8400S supplied by the company Brüker faculty of Pharmacy / University of kufa, Germany, At the university's Shahid Beheshti-Tehran, Iran, lab, **NMR** spectra were measured using a type of Bruker Ultra Shield 300 MHZ Switzerland (Dichloromethane) as just a solvent. Thermogravimetry analysis **(TGA)** was carried out between the range of temperatures ranging between 40 and 500 degrees Celsius using a heating rate of 10 degrees Celsius per minute in an argon environment. and Tehran, Iran, using the American PerkinSTA6000 **measuring instruments for differential thermal analysis (DSC)**, **USpicydownlight**, (CRESCENT, USND-1801 18W LED, American, **homogenizer**(korea),.Industry Heated Ultrasonic Cleaner Heat, **Scanning electron microscope** (SEM) TESCAN mira3(Geoslovkia) at Tehran Iran, **UV biochrom**118034, Ultraviolet-visible spectrophotometer, England , **PH-Meter**, OHAUS Corpation ,USA.

PREPARATION METHODS OF POLYMERS

Choose The Best Material For Crosslinking

DMA-Based Hydrogels' Polymerization

As a cross-linking agent, a total of (5) gm of DMA with various weights of (EGDMA, HDODA &TEGDA) (0.05, 0.1, 0.2, 0.3, 0.4, 0.6, 0.9, 1, 1.2) %. As a photo initiator, (0.05) gm of 1-hydroxycyclohexyl phenyl ketone (PI184) was used to start the polymerization process. To eliminate the oxygen, For 30 minutes, nitrogen was used to degas the reaction mixtures. The combination was blended for 30 min at room temp. Following pouring into polypropylene molds, the mixture was exposed to UV radiation below 365 nm till it hardened. The nanopolymers is then soaked in a liquid detergent consisting of 20% ethanol to for eliminating photoinitiator as well as unreacted monomers, After that, to rinse ethanol,0.6% is the best weight crosslinking ratio was chosen from other ratios and then it was compared with the rest of crosslinking type as the best cross-linking obtained was HDODA.

GENERAL METHOD OF SYNTHESIS FOR ALL NANOPOLYMERS HYDROGEL

Just (PLA,PVP and Cs) were dissolved in ethyl acetate, water and 1% acetic acid respectively, and other monomers didn't need that, At room temperature as described in Table(1). The monomers for hydrogels are Free-radical polymerization occurred while a crosslinking agent was present, HDODA and photo initiator PI184. To eliminate the oxygen, the contents of the flask were degassed with nitrogen for 30 minutes. then put the mixture under stirring with a homogenizer at a speed (3000 rpm) for 15 min. Stirring the emulsion at room temperature preceding homogenization at (12700) rpm for 15 min using an TOPS-SR30 homogenizer and Industry Heated Ultrasonic Cleaner Heat at temperature of (40 ºC). the mixture was placed in a mold and exposed to UV radiation below 365 nm till it hardened. then, the hardened polymer is then soaked in a liquid detergent consisting of 20% ethanol for eliminating photoinitiator as well as residual monomers. After that, to rinse the ethanol from the hardened polymer, For total formulas, the ratio from HDODA andP1184 were 0.6 weight percent and 0.05 weight percent, respectively.

Table(1) Formulations Of Nano Polymers Hydrogel By Monomers.

Sample	Monomer1 / Wight (mg)	Monomer2/ Wight (mg)	Monomer3/ Wight (mg)	Copolymerization	Time irradiation /min
1	PLA/20 mg	AA / 400 mg		(PLA-co-AA)	2
2	PLA/20 mg	AA / 200 mg	DMA/200 mg	(PLA-co-AA-co- DMA)	10
3	PVP /200	DMA/200	(BADMA)/50	(PVP-co-DMA-co-BADMA)	20
4	MMA /200	MA / 200	Cs /50	(MMA-co-MA-co-Cs)	25
5	EG/200	MA/200	PLA/50	(EC-co-MA-co-PLA)	15

ULTRAVIOLET (UV) MEASUREMENTS

Using a UV/Vis Spectrometer with the Biochrom LDT Model, the loaded and released amounts of the model drug Atenolol were determined at max 225 nm.

PH MEASUREMENTS

The preparation of buffer solutions range in concentration from (2, 4, 7 and 8) was accomplished by utilizing, respectively,((trisodium citrate/citric acid) with sodium dihydrogen phosphate/disodium hydrogen phosphate [15].

PREPARATION OF CALIBRATION CURVE

The wavelength is selected so that it falls on the center of the spectral abroad maximum. where just one component in the sample absorbs appreciably in order to reduce wavelength-setting errors. Two quantification methods are utilized, Assuming the Lambert-Beer law's linear range has been established and the drug concentration has been changed to fall within the ideal range for the instrument type in question.

If a reliable drug standard is provided, the calibration graph goes through zero, the standard is replicated, and the tests are conducted in brackets and at the same concentration, the standard is used (i.e. each group of samples is preceded and allowed by the standard). utilizing the same matched cells, under the same temperature and solvent conditions.

In the range of (0.008 -0.05g.l^{-1}), an Atenolol standard curve was designed. Using distilled water as the solvent, the Solutions were prepared from a stock solution. Regression study indicates a linear association between the concentration of Atenolol and the absorbance of the resultant solutions, which were measured for absorbance using a UV-Visible spectrophotometer at max 225.0 nm and distilled water as a blank.

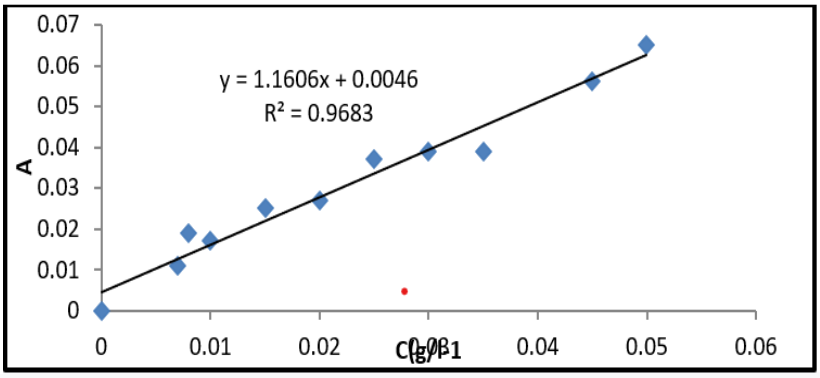

Figure (1) Calibration curve of Atenolol drug

SWELLING MEASUREMENT

All hydrogels' dynamic swelling characteristics were studied in double distilled water. Through the use of gravimetry, the equilibrium swelling was calculated. The swelling equilibrium was achieved by soaking the hydrogels (0.1gm) for 10 days at various temperatures (37 and 39 ^{0}C) in 100 ml of different pH solutions (pH=2, 4, 7 and pH=8). At regular intervals, the swollen gels were separated from the water and weighed after being lightly wiped to remove any additional surface water using filter paper. As a result, the amount of swelling was determined using the formula gram of water per gram of polymer (g/g) **[16].**

$$\text{Swelling Degree (g/g)} = (Ws - Wd)/100Wd \quad \ldots\ldots (1)$$

Where Ws and Wd represent the weights of the swollen gel and the dry sample at a given time..

LOADING DRUGS TO NANOPOLYMERIC HYDROGELS

Using the swelling equilibrium method, the drug was loaded onto the hydrogels that had been synthesized. The hydrogels were dried at room temperature after being allowed to swell in a known concentration of drug solution for 24 hours at pH (2, 4, 7andpH= 8). The drug percentage adsorbed in the polymer matrix was calculated by measuring the concentration of the rejected solution. **[17].**

RELEASE OF DRUG (ATENOLOL)

The amount of atenolol released from the hydrogel network is calculated using a loaded hydrogel sample. Where the sample was dried and weighed (100.300.500 mg) before soaking it in100ml of various solutions of pH (2,4,7and PH = 8) by adding 100mg of a atenolol drug at a temperature (37,39 °C) for ten days, the quantity of Atenolol released was measured utilizing a UV spectrophotometer at λ maximum 225 nm every day **[18].**

IN VITRO DRUG RELEASE STUDIES

Material And Methods

Male Wistar rats weighing 200–240 g were used for studying antihypertensive effects of the polymers. Animals were procured from Animal facilities of Shahid Beheshti University, Tehran, Iran and housed in cages in the Animal room of the faculty of life science and biotechnology for 7 days for further acclimation. Room temperature was maintained at 24 °C and controlled light (12h light /dark cycle) was used for lighting. Body weight and water intake were measured throughout the experimental treatments and divided with similar mean body weight. There was unlimited food and water available to animals. The care and use of animals for scientific reasons was adhered to throughout every animal procedure, according to SBU ethics.

In order to induce hypertension, Rats were first treated with Nacl (1%) in their drinking water. for a week followed by injection of 0.03 mg/kg/day Dexamethasone to each rat for 7 days according to the protocol described by Soto pina et al**[19]** with slight modification. Prior to start the main experiment, increased blood pressure of rats were confirmed. For the main evaluation, animals were randomized into six treatment groups of 3 animals per group ($n = 3$) as follows:

- NT – Control.
- Polymer 1+ Atenolol (3) (PVP-co-DMA-co-BADMA)+ Atenolol)
- Polymer 2+ Atenolol (4) (MMA-co-MA-co-Cs)+ Atenolol)
- Polymer 3+ Atenolol (1) (PLA-co-AA)+ Atenolol)
- Polymer 4+ Atenolol (5) ((EC-co-MA-co-PLA)+ Atenolol)
- Polymer 5+ Atenolol (2) (PLA-co-AA-co- DMA)-AA)+ Atenolol)

For preparation of the treatments 2-6, 0.3g of Atenolol dissolved into 20cc Sterile deionized water and consequently added into 0.1g of each milled polymer according to the protocol described by Tonolo et al **[20]** and kept for 24h. All treatments above were given for 4 weeks every day through Oral gavage in order to feed equal volume of an agent to each rat directly into their stomach.

MEASUREMENT OF SYSTOLIC BLOOD PRESSURE

On the seventh day of the experiment, the blood pressure of the Wistar rats was measured using the non-invasive tail-cuff method described by Imanshadi et al., 2015**[21].** Then, to enhance blood flow to the tail, The rats were first heated for about 15 minutes at 30 degree and then blood pressure was measured with cuff invasive tail cuff technique at the proximal end of the animal tail (Model 29 SSP, Harvard Apparatus, Montreal, Canada) [**22**]was used to measure blood once a week until the study's conclusion.

The final blood pressure reading was calculated by averaging three separate measurements, which were done three times. The tail cuff pressure was raised above tail artery occlusion pressure after enabling the animals to get used to the restrainer. When there was no longer any pressure in the tail cuff, pressure was gradually released from the cuff. In order to give the tail artery time to rest between readings, this process was done every 30 to 60 seconds. The corrected SBP was found for every reading. As the cuff pressure was released, raw SBP was measured at the location where pulse channel deflections started to occur once more. The mean value of the five seconds prior to the start of the reading is used to determine baseline pressure once the raw SBP data has been collected. The corrected SBP was determined by using the raw and baseline pressures.as follows:

Corrected pressure = Raw systolic blood pressure –Baseline pressure.

ANALYTICAL STATISTICS

One way ANOVA for repeated measures was used for all statistical analyses. T-tests were performed to compare two measurements individually. The standard error of the mean was used to express all data (SEM). Statistics were considered accurate if the P value was less than 0.05.

RESULTS AND DISCUSSION

Nanocopolymer Synthesis And Characterization

When **(PLA)** and **(AA)** were copolymerized, was synthesized **(PLA-co-AA)** . Was also synthesized **(PLA-co-AA-co-DMA)** by copolymerization of **(PLA**), **(AA)**, with (**DMA)**.Also **(PVP-co-DMA-co--(BADMA))** was synthesized by copolymerization of **(PVP)**, **(DMA)** with **(Bisphenol A dimethacrylate)**. Where **(MMA-co-MA-co-Cs)** was synthesized by copolymerization of **(MMA)**, **(MA)** with **(Cs)**. Finally, **(EC-co-MA-co-PLA)** was synthesized by copolymerization of **(EC**), **(MA)** with **(PLA)**. Using 1-hydroxycyclohexyl phenyl ketone as photoinitiator and HDODA like a crosslinking agent The reaction mixture was stirred at room temperature for 30 minutes. while nitrogen was purged through it to get rid of any dissolved oxygen. The mixture was radiated under 365 nm UV light for 2,10,20,25

and 15 minutes, respectively . after being poured into polypropylene molds. Schemes shown this reaction (1,2,3,4 and 5).

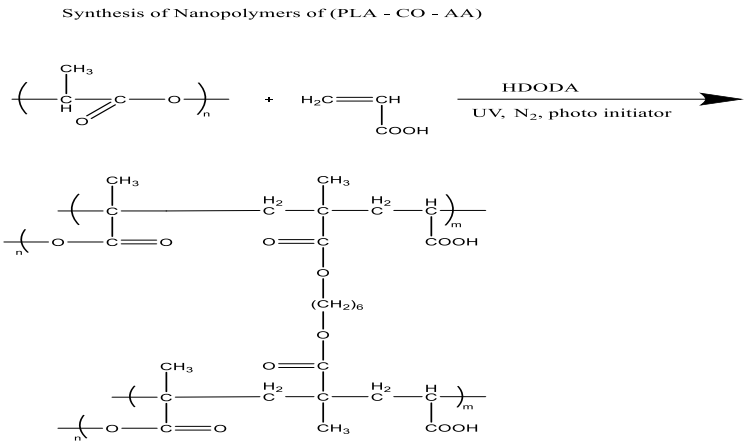

Scheme 1: Synthesis of nanopolymer (PLA-co-AA)

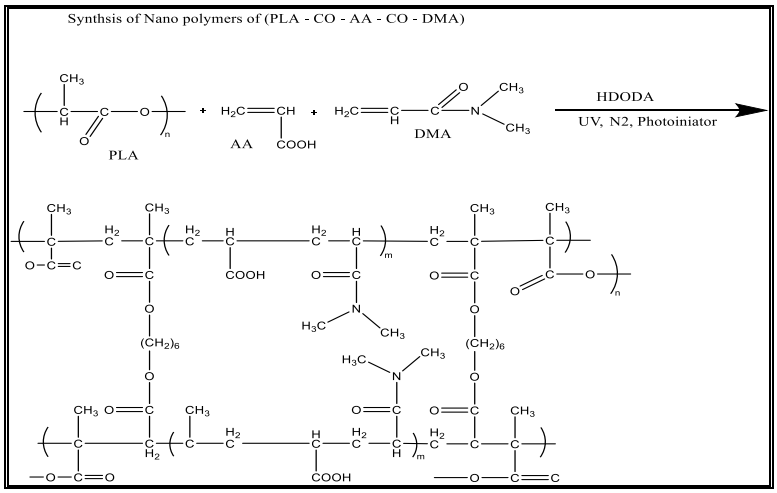

Scheme (2): Synthesis of polymer (PLA-co-AA-co-DMA)

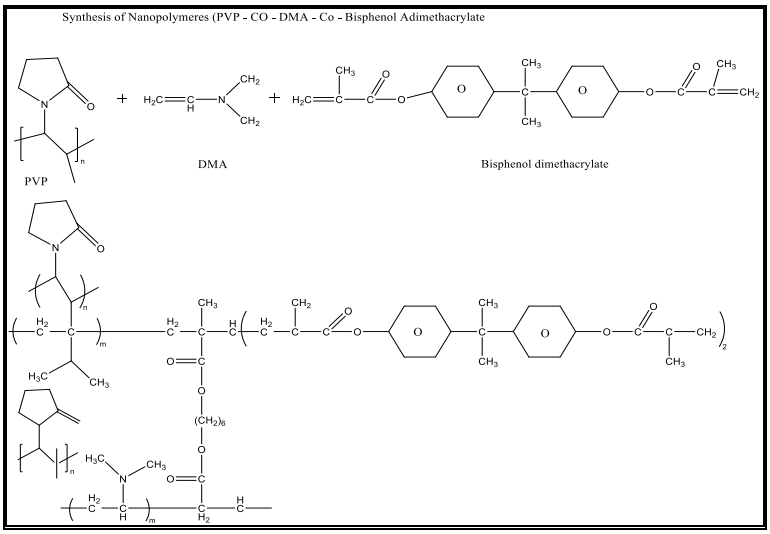

Scheme (3): Synthesis of polymer (PVP-co-DMA-co- (BADMA))

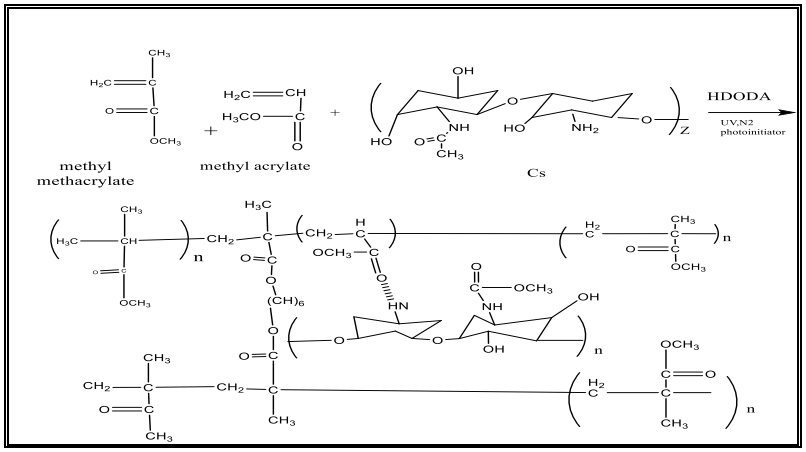

Scheme (4): Synthesis of polymer (MMA-co-MA-co-Cs)

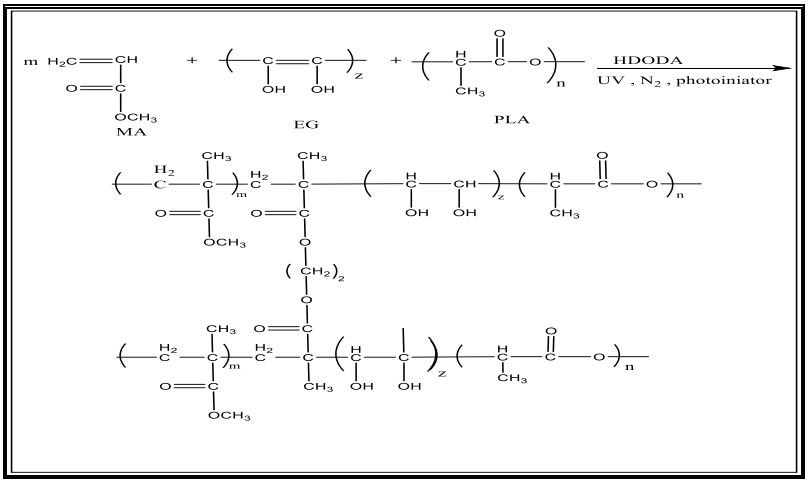

Scheme (5): Synthesis of polymer (EC-co-MA-co-PLA)

FTIR Spectrum

Figure (2)demonstrates the (PLA-co-AA) FTIR spectrum. It has absorption bands at 3000-3641cm^{-1} because of the polymer's (-OH str. group), 2949 cm^{-1} because of its (C-H str. Backbone of Aliphatic Polymer), 1732cm^{-1} because of its (C=O str., ester group), 1614cm-1 because of its (C=O str. carboxyl group), and 1178cm-1 because of its (C=O str (-C-O of C-OH str.).The valence vibrations of the symmetric and asymmetric C-H from CH_3 are represented by bands in the PLA spectrum at 2395 and 2274cm^{-1}, respectively . At 1614 and 1597 cm^{-1} The band shift in the polymer is caused by the C=O st. The arrangement of molecules in the polymer chain is indicated by the difference in peak intensities in these bands that demonstrate monomer to polymer shifts. Bands corresponding to CH3 bending vibrations (symmetric and asymmetric) in the polymer spectra were observed as higher intensity peaks than those from the monomer at 1408 and 1476 cm^{-1}. Asymmetrical and symmetric valence vibrations of C-O-C were discovered at 1274cm^{-1}. Additionally, the presence of unreacted monomers was indicated by the full disappearance of bands that are characteristic at approximately Vinyl groups of the monomers at (900 cm^{-1} - 3100 cm^{-1}) entirely vanished, indicating the absence of unreacted monomers. [23–25].

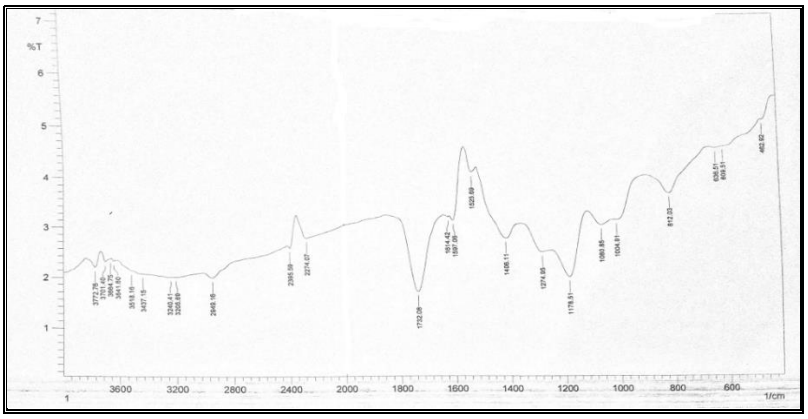

Figure 2: FTIR Spectra of (PLA-co-AA)

Figure (3) illustrates the FTIR spectrum of PLA-co-AA-co-DMA, which represents absorption bands between 3400 and 3437 cm^{-1} because of the polymer's (-OH str. group), 2943 $cm^{-1}$and 2817 cm^{-1}back to (C-H str. aliphatic polymer backbone), 1603 cm^{-1} to (C=O str. carboxyl group), 1734 cm^{-1} to (C=O str. ester group), 1166 cm^{-1} to (C-O- of C-OH str.). The PLA spectra bands at 2617 and 2360cm^{-1} correspond to symmetric and asymmetric valence vibrations of C-H from CH_3, respectively. It is possible to see a band shift connected to the C=O stretch in the polymer to 1734cm^{-1}. The peak intensity of these bands that demonstrate the transition from monomer to polymer varies, which may indicate the arrangement of the molecules along the polymer chain. Bands corresponding to bending vibrations of CH3 (asymmetric and symmetric) were observed as higher intensity peaks in the polymer spectrum at 1493 and 1531 cm^{-1} than in the monomer at 1408 and 1476cm^{-1}. The symmetrical and asymmetrical valence vibrations of C-O-C were discovered at 1257 and 1166 cm-1, respectively. The stretching vibration of the C-O-C is found at 1333cm^{-1}. Further evidence of the absence of unreacted monomers was provided by the full disappearance of distinctive bands at approximately 900 $cm^{-1}$and 3100 cm^{-1}, which correspond to the vinyl groups of monomers. The amide band for N'N-dialkyl substituted amides is in the range of 1608 cm^{-1}. With modest contributions from the C-N stretching mode, the C=O stretching mode is primarily responsible for the amide band at 1629 cm^{-1}. In this study, the symmetric stretching modes of the N(CH3)2 group were assigned to the polarized band at 1058 cm^{-1}. **[23-25]**.

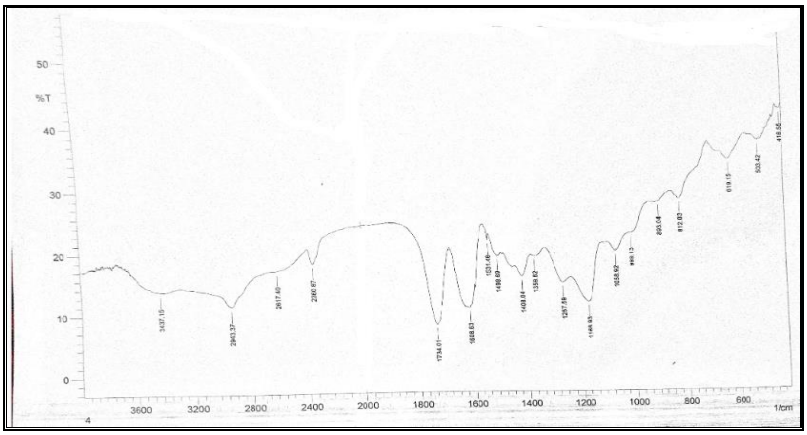

Figure (3): FTIR Spectra of (PLA-co-AA-co-DMA)

Figure (4) depicts the FTIR spectrum of **(PVP-co-DMA-co-Bisphenol A dimethacrylate**), which exhibits absorption bands at 3456 cm-1 due to the polymer's (-OH str. group); 2935 cm-1 as a result of (C-H str. of polymer backbone); 1700 cm^{-1} due to (C=O str., ester group); 1666 cm^{-1} due to (-N-C=O); 1500 cm^{-1}, 1433 cm^{-1}, and 13 (C-O-C str.). 1064cm^{-1} to (C-N str.) totally vanished, indicating that there were no unreacted monomers present. The amide band is seen for N'N-dialkyl substituted amides in the range of 1620-1670 cm^{-1}. With modest contributions from the C-N stretching mode, the C=O stretching mode is primarily responsible for the amide band at 1637cm^{-1}. This analysis assigned the symmetric stretching modes of the N(CH3)2 group to the polarized band at 1064 cm^{-1} **[23-25].**

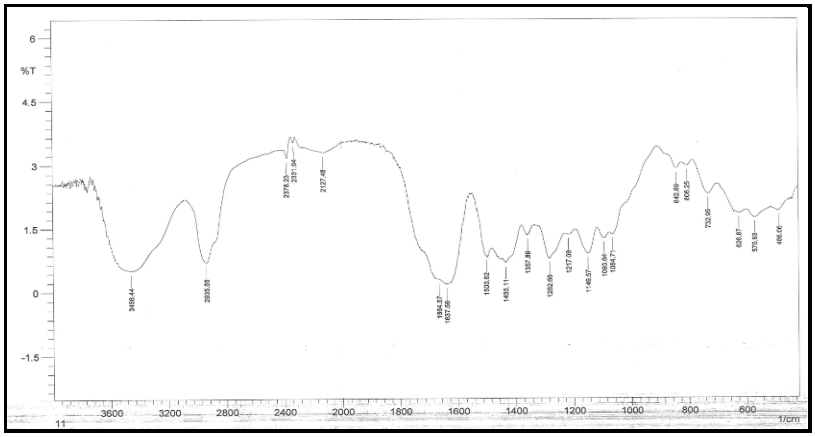

Figure(4): FTIR Spectra of (PVP-co-DMA-co- (BADMA))

The FTIR spectrum of (MMA-co-MA-co-Cssynthesis)'s and characterisation is depicted in Figure (5), and it shows absorption bands at 3344 cm^{-1} due to the polymer's -OH str. group, 3292 cm^{-1} due to the N-H str. of Cs, 2941 cm^{-1} due to the polymer backbone, and 1703 cm^{-1} due to the(C=O str. ester group), 1622 cm^{-1} to (N-H-C=O) 1164cm^{-1}, 1095cm^{-1} to (C-O-C str.),1064cm^{-1} to (-C-O of C-OH str.), 1180cm^{-1} to (C-N str.), and 2719cm^{-1} to C-CH_3 **[23–25].**

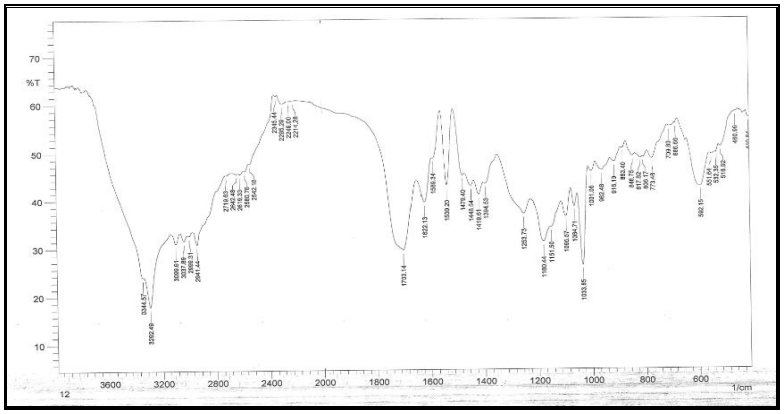

Figure (5): FTIR Spectra of (MMA-co-MA-co-Cs)

Figure 6 illustrates the FTIR spectrum of the compound (EC-co-MA-co-PLA), which shows absorption bands at 3375 cm^{-1} (due to the polymer's -OH str. group), 2943 cm^{-1}, 2881 cm^{-1} (due to the compound's C-H str. Aliphatic polymer backbone), 1722 cm^{-1} (due to the compound's (C=O str. ester group), 1161 cm^{-1} (due to the compound (-C-O of C-OH str.). A band shift connected to the C=O stretch in the polymer to 1722cm^{-1} can be seen. The peak intensities of these bands that demonstrate the transition from monomer to polymer varies, which may indicate how the molecules are arranged along the polymer chain. In comparison to the monomer peaks at 1408 and 1476 cm^{-1}, In the polymer spectra, bands corresponding to the bending vibrations of CH3 (asymmetric and symmetric) were observed at 1392 and 1454 cm^{-1}. At 1273 and 1247cm^{-1}, respectively, C-O-C symmetrical and asymmetrical valence vibrations were discovered; the stretching vibration of C-O-C was found at 1392cm^{-1}. Further evidence of the absence of unreacted monomers was provided by the full disappearance of typical bands at roughly 900 cm^{-1} and 3100 cm^{-1}, which corresponded to the vinyl groups of monomers **[23-25]**.

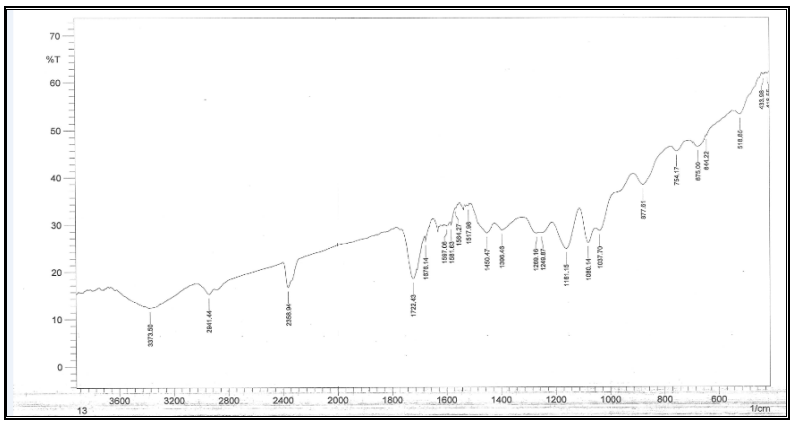

Figure (6): FTIR Spectra of (EC-co-MA-co-PLA)

^{1}HNMR SPECTRUM

1HNMR spectrum of (PLA-co-AA), is shown in Figure (7); (s,(1.2-1.8)δ ppm) for (3H,CH_3), d (4.35 δ ppm) corresponds to the methine linked to the end group –OH(s,4.1 ppm) for (2H,COOCH2,HDODA),and (s,5.3 ppm) as a result of (1H,COOH) **[23-25].**

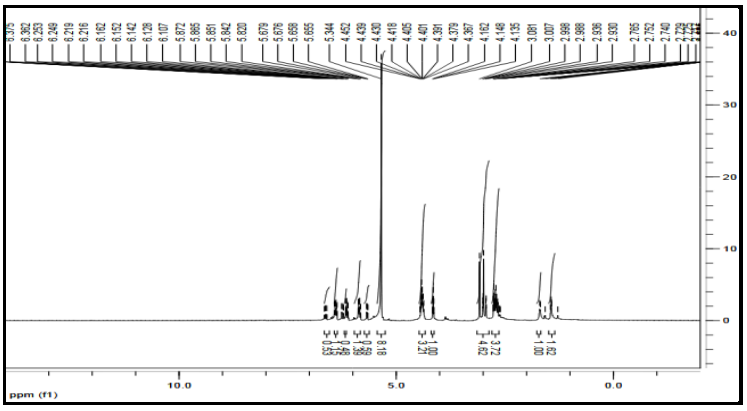

Figure 7: 1HNMR Spectra of nanopolymer (PLA-co-AA)

[1]HNMR spectrum of (PLA-co-AA-co-DMA), is shown in Figure (8); (s, δ (0.95)ppm) for (3H,CH_3), δ(4.5) ppm(s,2H) for (C-H),(s, (4.1) ppm for (2H, COOCH2, HDODA), (s, (5.3)ppm for (1H, COOH), and (s, (3.8) ppm for (N-CH3) **[23-25]**.

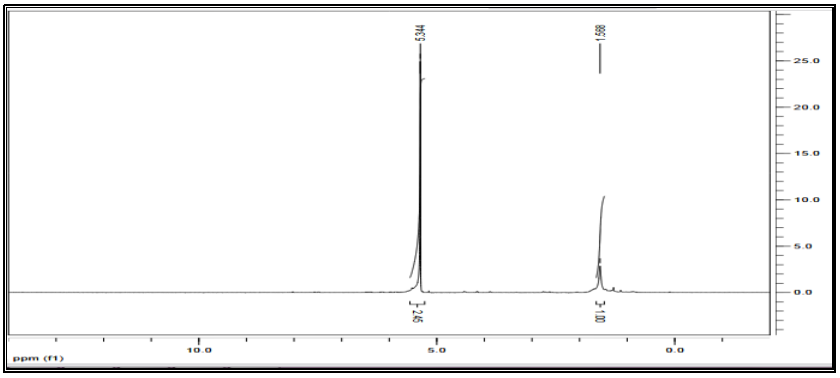

Figure (8): 1HNMR Spectra of nanopolymer (PLA-co-AA-co-DMA)

[1]HNMR spectrum of (PVP-co-DMA-co-Bisphenol A dimethacrylate), is shown in Figure (9); (s,1.5δ ppm) for (2H,CH2 HDODA),(s,2.4 ppm) for (-CH_2-CO-N pyrrolidone ring),(m,2.7-2.9 δ ppm)for (-CO-CH_2-COHDODA),(s,3.52 δ ppm) for (–CH_2-C-N),(m,3.1-3.2 δ ppm) for (2H,O-CH_2 Bisphenol A dimethacrylate),(m,5.0-5.3 δ ppm) for (COO-CH_2 HDODA)**,** a multiplet at (2.6 δ ppm) to (6H, N-CH_2) **[23-25]**.

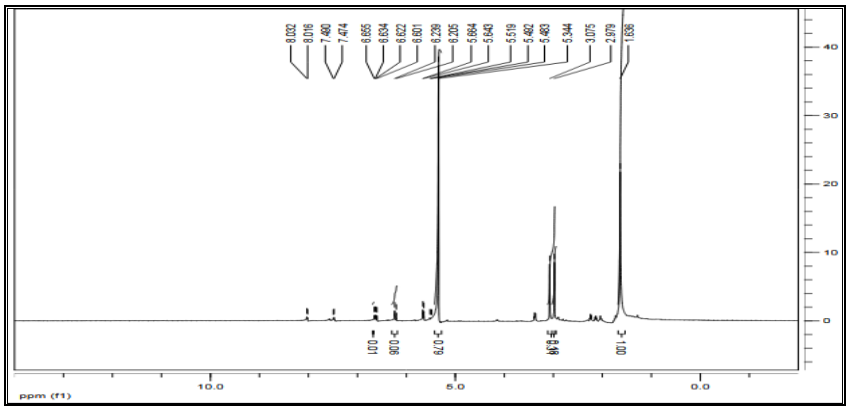

Figure (9): 1HNMR Spectra of nanopolymer (PVP-co-DMA-co- (BADMA))

[1]HNMR spectrum of Synthesis and Characterization of **(MMA-co-MA-co-Cs)**,is shown in Figure (10);(s,1.2δppm)for(3H,CH_3 H for(3H,CH_3 MA; CH_3,HDODA),(m,1.3-1.8δ ppm) for (2H,CH_2 MA;CH_2 HDODA),(s,2.1 δ ppm) for (3H $COCH_3$), (s,3.4 δ ppm) for (1H OH Chitosan),(m,4.2δ ppm) for (2H,COOCH2,HDODA), (s,6.5δ ppm) for (1H,NH Chitosan) **[23-25].**

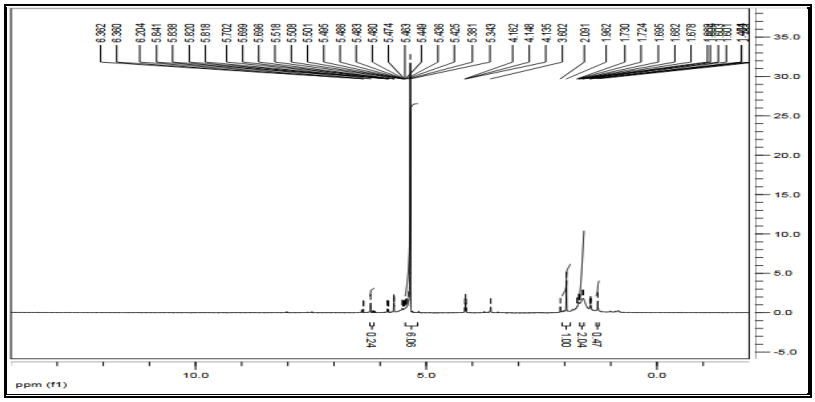

Figure (10): 1HNMR Spectra of nanopolymer (MMA-co-MA-co-Cs)

Figure (11), which depicts the 1HNMR spectra of **(EC-co-MA-co-PLA),** includes the following values: (s,1,65 ppm) for (3H,CH3), (s,2.5 ppm for (2H), (s,3.5 ppm for (2H,COOCH2,HDODA),and(s,5.5ppm)for(1H,OH)**[23-25].**

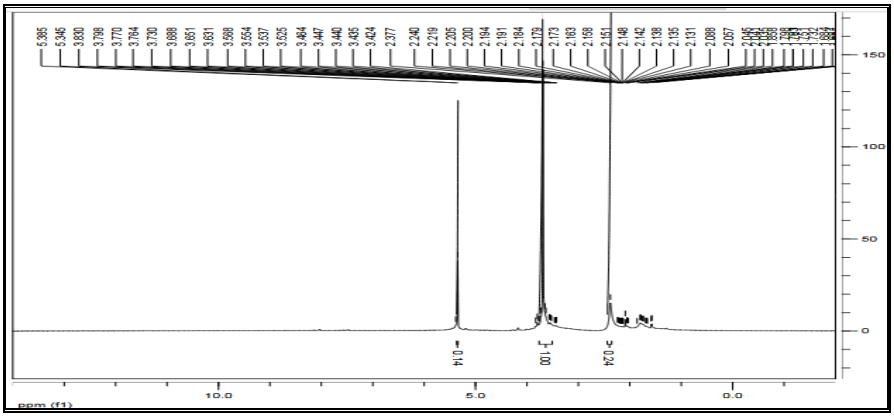

Figure (11): 1HNMR Spectra of nanopolymer (EC-co-MA-co-PLA)

SCANNING ELECTRON MICROSCOPY (SEM)

To identify the nature of the surface structure (surface topography) of the research material, a (SEM) examination of the nanopolymer was carried out. The morphology and geometry of the created nanopolymer's surface were determined using scanning electron microscopy (SEM), which revealed a smooth surface and a distinct network throughout the structure. Figures (12–16) show that the porous surface of polymers, particularly MIP, could be clearly seen.

This test shows the shape and size of nanopolymer at two magnifications of 200 nm and 500 nm. These images show the structure of the nanopolymer and its multiple layers.

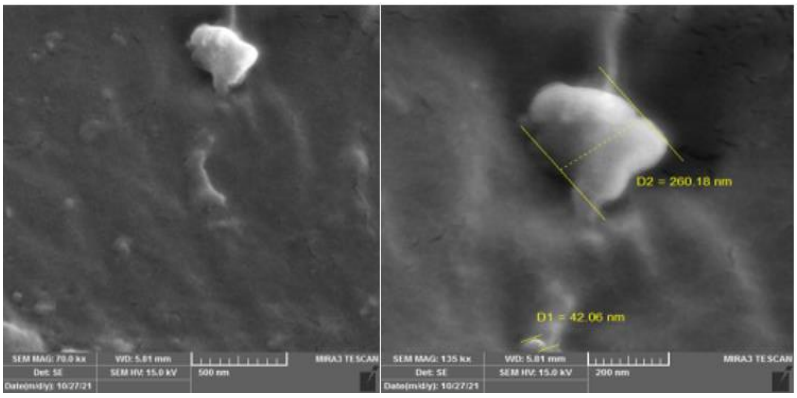

Figure(12) FESEM micrograph of (PLA-co-AA)

showed a clear network and smooth surface throughout the structure. Additionally, as illustrated in Figure, the porous surface of polymers, particularly MIP, could be clearly seen (13).

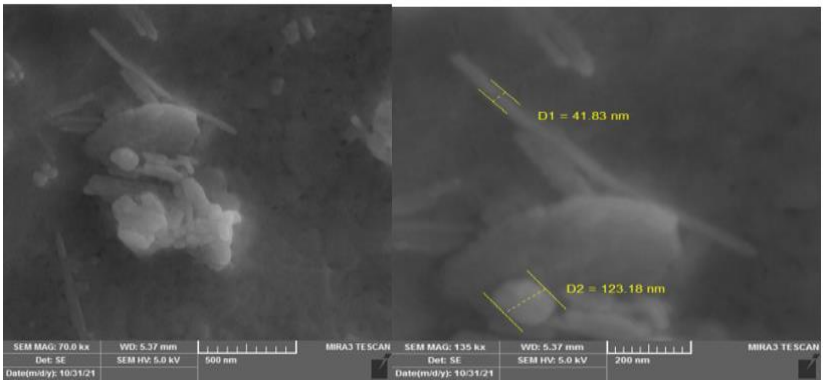

Figure (13): FESEM micrograph of (PLA-co-AA-co-DMA)

It is noticeable that each particle is almost spherical. These photos demonstrate the variations in agglomerations that occur in different particle types; the more particles present, the more agglomeration takes place. These images allow us to deduce that there is more particle to particle interaction as the number of particles increases, as illustrated in Figure (14).

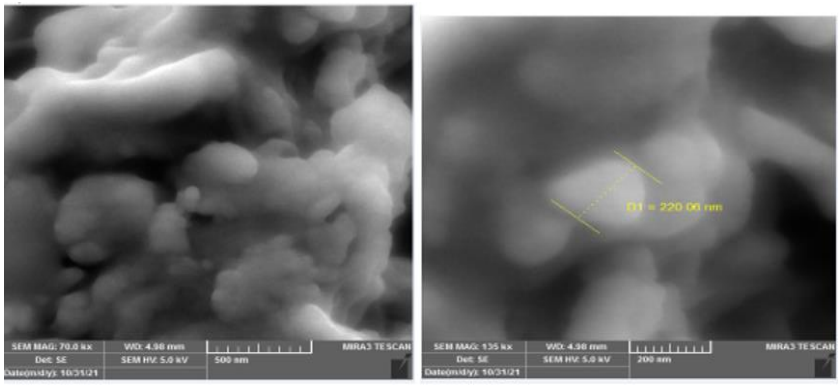

Figure (14): FESEM micrograph of (PVP-co-DMA-co- (BADMA))

It is observed that the nanopolymer (MMA-co-MA-co-Cs) afforded perfect dispersion. The reason is that the smaller sizes of nanoparticles tend to agglomerate easily. Consequently, having nanopolymer (MMA-co-MA-co-Cs) steric hindrance between nanoparticles and prevented their aggregation. It is thus concluded that the nanoparticles of nanopolymer of (MMA-co-MA-co-Cs) had a better dispersion property as shown in Figure (15).

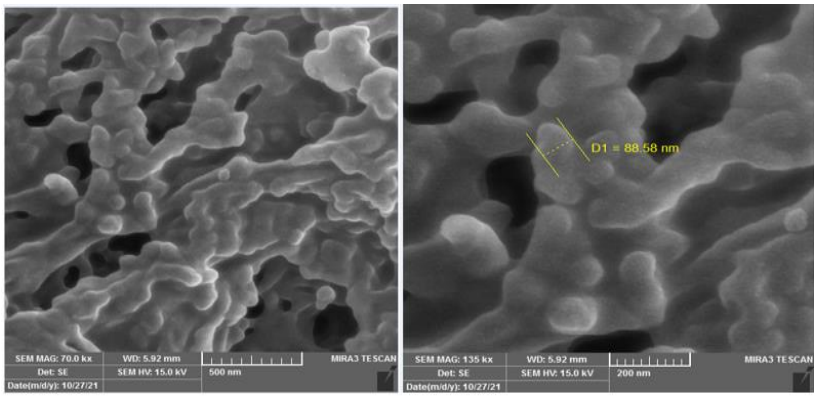

Figure(15): FESEM micrograph of (MMA-co-MA-co-Cs)

The individual particles are shown to be almost spherical. However, depending on the support, the degree of spherical particle agglomeration varies. Figures illustrate how nanoparticles exhibit equally scattered particles with little aggregation (16).

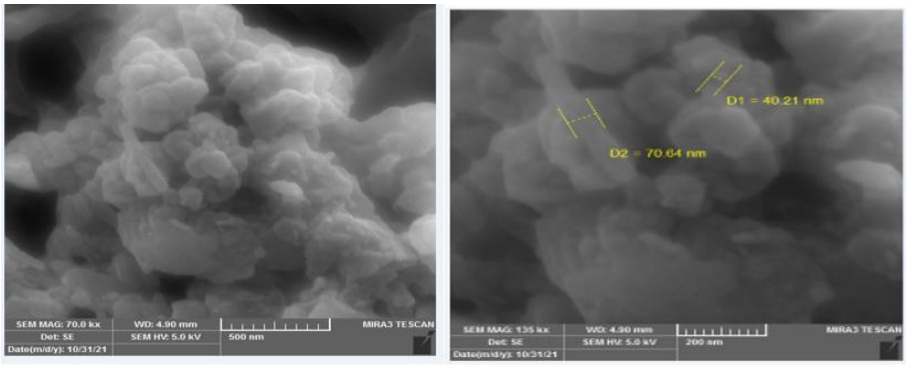

Figure(16): FESEM micrograph of(EC-co-MA-co-PLA)

THERMAL PROPERTIES

Analysis Utilizing Thermo Gravimetric Techniques (TGA)

Analysis using thermo gravimetry (TGA) is the method of calculating mass changes solely as a function of temperature. When describing degradation temperatures, the quantity of absorbed material , the proportion of organic and inorganic components in a sample, as well as the residues analytical solvents leave behind. A sensitive electronic balance is used to keep the sample suspended in a furnace that is controlled by a temperature regulator. The thermal properties were investigated using TGA for five samples of these polymers in an argon environment, at a heating rate of 10 ^{o}C/min **[26-29].** Several values were identified in this test, includes char yields at 400 °C and % residue at 500 °C, Ti, Top, Tf, and T50 %. respectively as demonstrated by data in the (Table 2).

Table 2: Some thermal stability properties of TGA curves for nanopolymers

Nanopolymers	TGA				$T_{50\%}$	Residue at500 C°	Char % *at* 400°C
	T_i	T_{op1}	T_{OP2}	T_f			
(PLA-co-AA)	155	225	285	500	265	8	26
(PLA-co-AA-co-DMA)	125	210	315	500	375	8	40
(PVP-co-DMA-co--(BADMA))	40	155	360	500	410	6	48
(MMA-co-MA-co-Cs)	90	190	310	500	410	12	50
(EC-co-MA-co-PLA)	70	200	330	500	355	2	30

Decomposition temperature is abbreviated as DT.
Ti: Starting temperature for decomposition.
Top: The ideal temperature of decomposing..
Tf: Final temperature of decomposing. temperature of decomposing at its peak
T50%: A 50% weight loss as a result of TGA temperature.
At 400 °C, % TGA Char
% of residual weight in argon at 500 °C

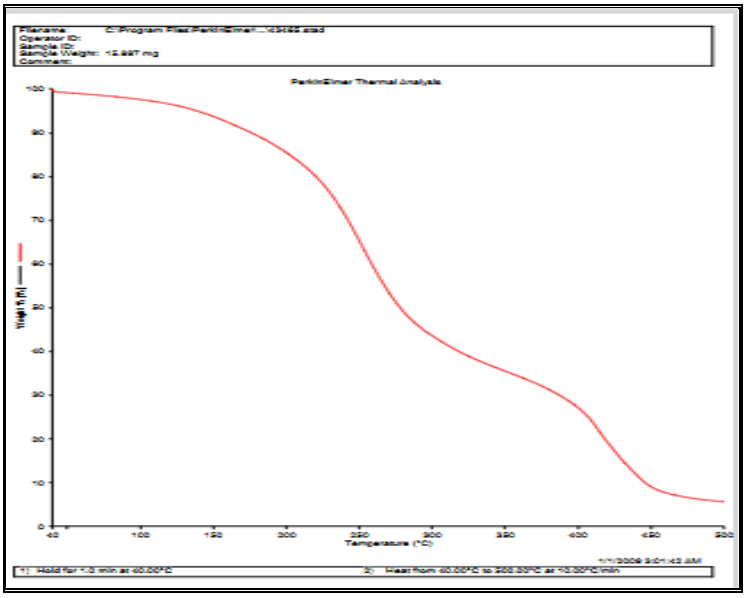

Figure 17: (TGA) curves for polymer (PLA-co-AA)

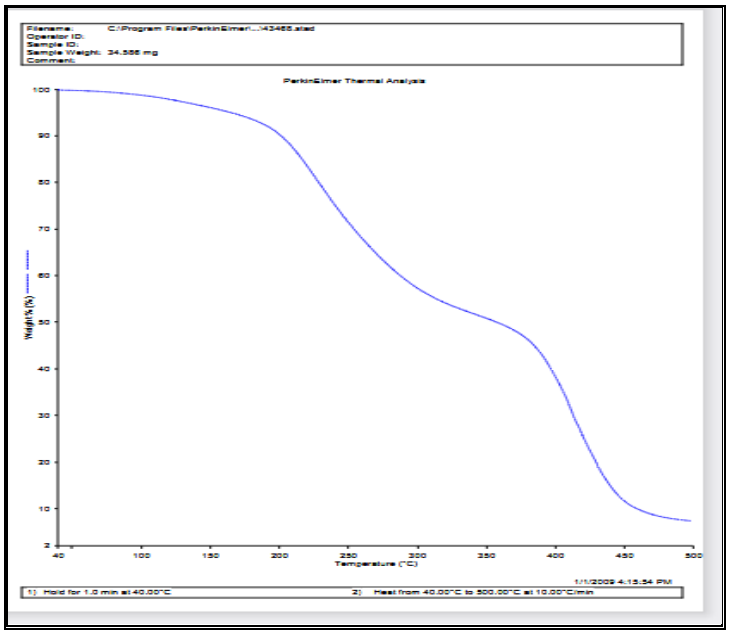

Figure18:(TGA) curves for polymer (PLA-co-AA-co-DMA)

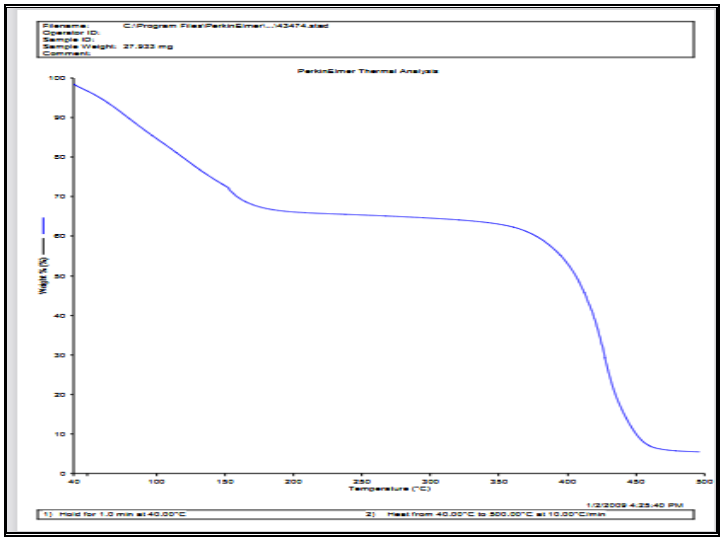

Figure19:(TGA) curves for polymer (PVP-co-DMA-co-(BADMA)

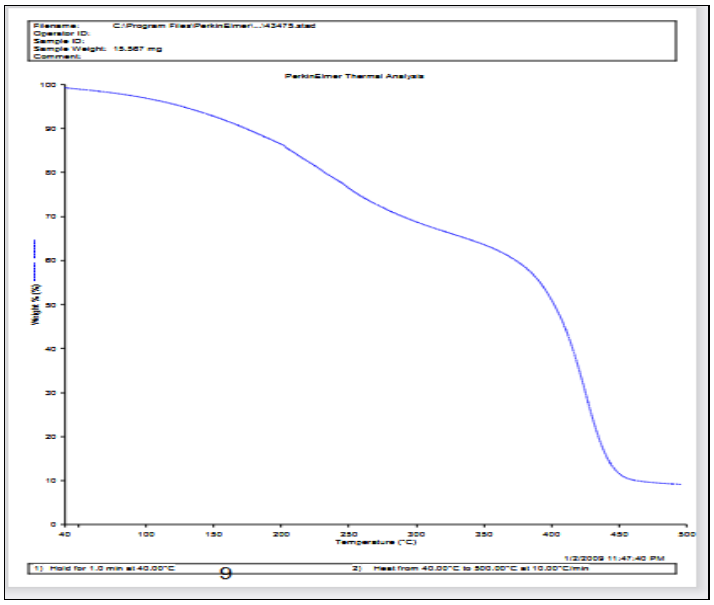

Figure20:(TGA) curves for polymer (MMA-co-MA-co-Cs)

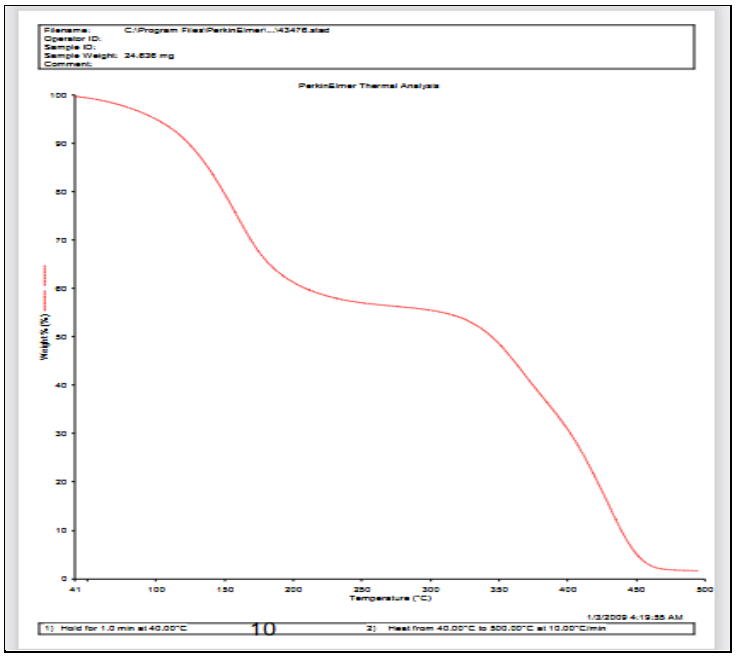

Figure 21:(TGA) curves for polymer(EG-co-MA-co-PLA)

Differential Scanning Calorimeter Analysis (DSC) Study

The amount of energy that a sample absorbs or releases as it is heated, cooled, or maintained at a fixed temperature is measured by DSC. It is accomplished by inserting two temperature probes into the furnace, measuring both the sample temperature and the temperature of the furnace at the same time, and heating the sample steadily. It is a method of thermal analysis that looks at how temperature affects a material's heat capacity (Cp). When a known mass sample is heated or cooled, changes in the heat flow can be seen as a result of differences in the sample's heat capacity. This makes it possible notice transitions such (Tg), (Tm), and (Tc) **[30].**Applications involving polymers and pharmaceuticals use this approach. The results of nan polymer showed The curve of a sharp exothermic peak in figure (22-26) .It can also be seen Tg, Tm, and Tc in the Table(3)

Table (3): shows the degree of glass transition, melting point and degree of crystallization in DSC

Samples	Tg (cº)	TM (cº)	TC (cº)
(PLA-co-AA)	**275**	**425**	**296**
(PLA-co-AA-co-DMA)	**120**	**440**	**160**
(PVP-co-DMA-co- (BADMA))	**115**	**385**	**210**
(MMA-co-MA-co-Cs)	**180**	**370**	**290**
(EG-co-MA-co-PLA)	**170**	**375**	**225**

Glass transition degree(Tg)
Melting Point (TM)
Crystallization degree(Tc)

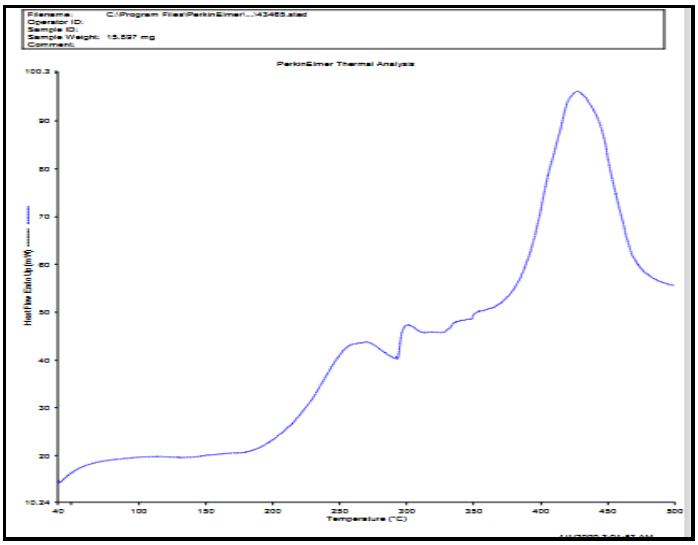

Figure 22: Curves (DSC) For Polymer (PLA-Co-AA)

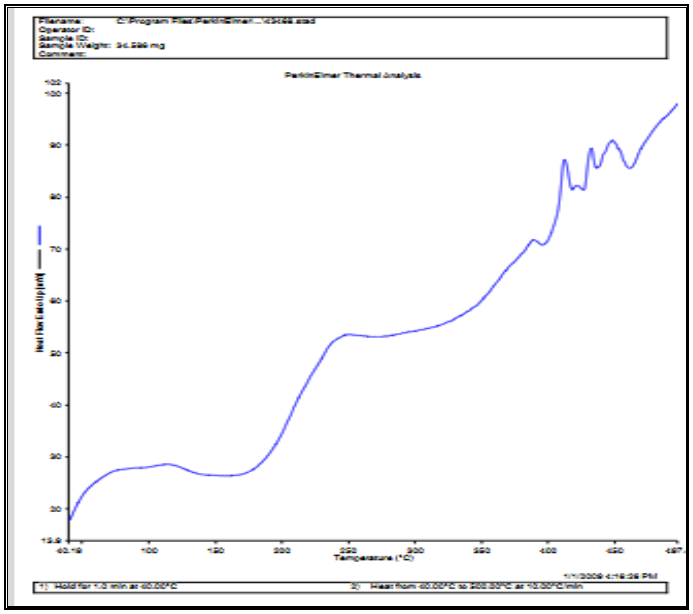

Figure23: Curves (DSC) For Polymer (PLA-Co-AA-Co-DMA)

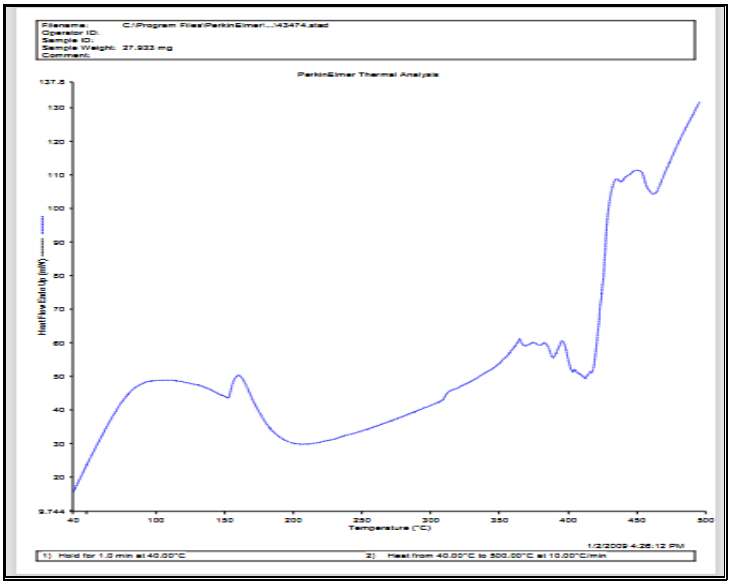

Figure 24: Curves (DSC) For Polymer (PVP-Co-DMA-Co- (BADMA))

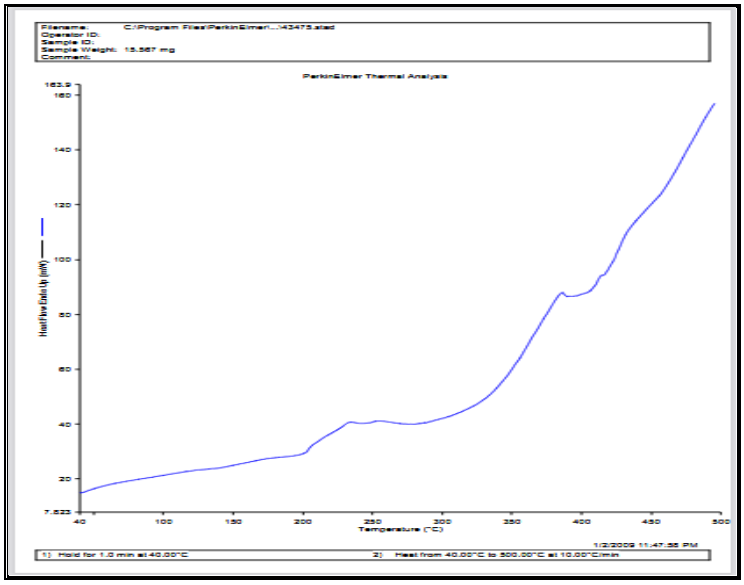

Figure 25: Curves (DSC) For Polymer (MMA-Co-MA-Co-Cs)

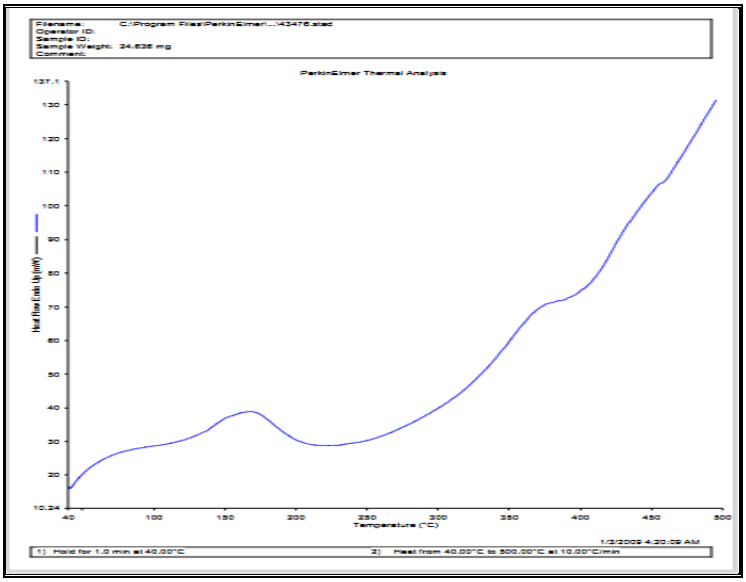

Figure 26: curves (DSC) for polymer (EG-co-MA-co-PLA)

THE INFLUENCE OF PH ON THE EQUILIBRIUM SWELLING OF THE NANOPOLYMER

The external solution's ionic strength and charge number have a major impact on the swelling ratio, as well as the nature of the polymer, which includes the network's flexibility, the degree of crosslinking density and the presence of hydrophilic functional groups. All five hydrogels' swelling ratio behavior at 37 ^{0}C was studied in relation to time and pH. Crosslinks dramatically decreased a polymer network's ability to absorb water. Figure (27) shows the swelling to time at various levels of pH for **(pLA- co– AA).**The swelling behavior of poly acrylic acid hydrogels depends significantly on the pH of the surrounding media owing to the carboxylic acid side groups. The PAA's carboxylic acid groups became more and more ionized as the media's pH increased. The hydrogels swelled more quickly in these circumstances via osmotic pressure caused by various ion concentrations in the ionic network and the surrounding solution between the ionized acid groups, electrostatic repulsion and electrostatic attraction [**31].**

Figure (28) represents the swelling to time for different pH for **(PLA-co-AA-co-DMA)**. The swelling of the resultant nanocopolymer increases with increasing PLA, (AA) and(DMA) concentrations. The nanocopolymer must be ionized after it has been synthesized (i.e; the hydrogen atom in the carboxyl group is removed). The carboxyl group is transformed (CO_2H) to the more hydrophilic ionized form (the carboxylate anion, CO2-) cause the water content to rise. This is frequently accomplished by nanocopolymer with sodium hydroxide, which neutralizes the carboxylic acid groups. However, because of their negative charges, carboxylate ions repel one another, a process known as "expanding the network." As a result, the network is able to absorb more water. The material would have a network that had not expanded if the nanocopolymer had not been ionized. DMA's amide group adds more hydrogen bonding sites for water. As a result, the hydrogels with a higher DMA content were shown to have a higher affinity for water **[32]** .The swelling to time for various pH levels is depicted in Figure (29) for **(PVP-co-DMA-co-(BADMA))** DMA is more hydrophilic than Bisphenol A dimethacrylate(BADMA) . Through increasing the amount of methyl methacrylate the water content of the (BADMA) can be reduced because these hydrophobic monomers contain numerous methyl groups, which reduce swelling behavior and the polymer network's expansion water content while keeping the chain rigid in the hydrogel that results **[33]**. As predicted, the amide group of DMA provides more hydrogen bonding sites for water than Bisphenol A dimethacrylate; thus, hydrogels with a higher DMA content have a higher affinity for water. Higher zwitterionic sulfobetaine monomer content in hydrogel resulted in greater swelling because the sulfobetaine unit could interact with water via both electrostatic forces and hydrogen bonds, providing a stronger water affinity than Bisphenol A dimethacrylate. **[32].** These polymers have a high water content due to the polar lactam moiety of (PVP), which is a benefit of the nonionic monomers (PVP), and the hydrophilicity of the polymer is increased by the presence of the polar lactam group in the pyrrolidone moiety. The carbonyl group offers two sites for the hydrogen bonding of water, which causes this rise.

Also, Figure (30) shows the swelling in time for the different pHs of **(MMA-co-MA-co-Cs).** The hydrophobic monomers MMA and MA include several methyl groups, which render The swelling behavior and water expansion of the polymer network are extremely poor, resulting in an inflexible chain in the resulting hydrogel, allowing for a reduction in the water content of hydrogels **[33].** As well since chitosan contains (-OH) groups that can form hydrogen bonds with water molecules, adding chitosan increases the water content of the hydrogel. This demonstrates that the hydrophilic monomer is being used to increase a hydrogel's ability to absorb more water **[34].**

Finally, Figure (31) shows the swelling in time for the different pHs of **(EG-co-MA-co-PLA).** The water content of hydrogels can be reduced by increasing the amount of MA because these hydrophobic monomers contain many methyl groups, which make swelling behavior and polymer network expansion water very poor and keep the chain rigid in the resulting hydrogel **[33].** EG is more hydrophilic than MA because the polymer contains two hydroxyl groups; the combined effect of EG and MA produces a high water content because EG can form hydrogen bonds with water molecules, increasing water content; clearly, the water content of a hydrogel material is related to the number of hydrophilic sites in the polymer **[35].** The swelling behavior of the hydrogels is highly dependent on the pH of the surrounding medium due to the carboxylic acid side group of PLA. The carboxylic acid groups on the PLA became increasingly ionized in higher pH medium. Because of the large swelling force caused by electrostatic repulsion between the ionized acid groups and the osmotic pressure caused by different concentrations of free ions within the ionic solution and the surrounding solution, the hydrogels swelled more quickly in these cases **[36].**

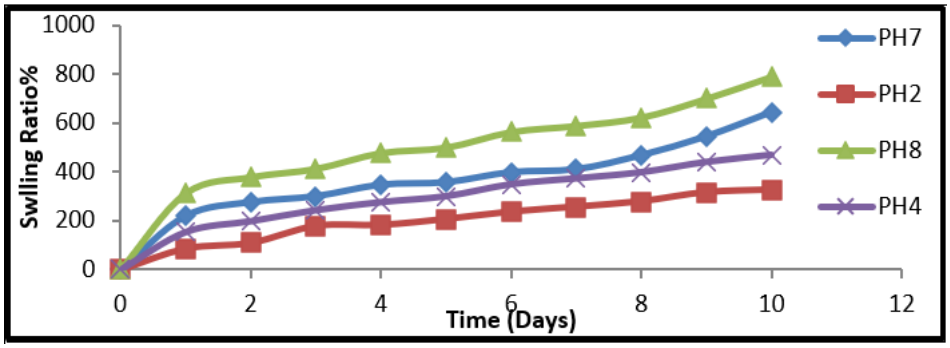

Figure(27): Swelling Ratio (Rs) For(Pla – AA) At Time Within Different Ph Range.

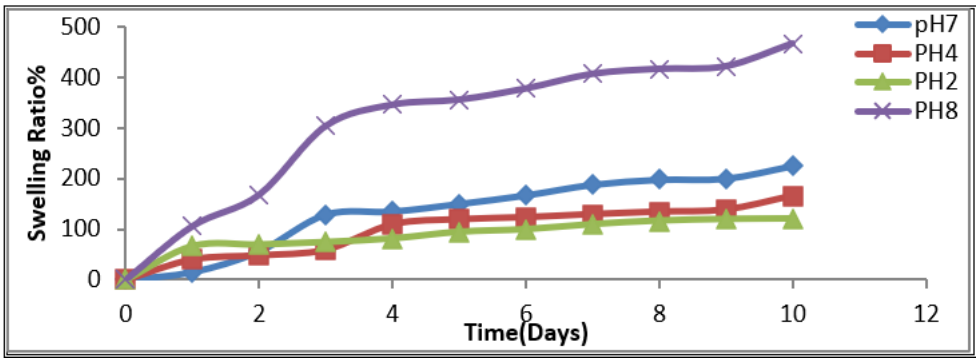

Figure (28): Swelling ratio (Rs) for (PLA-co-AA-co-DMA) at time within different pH range.

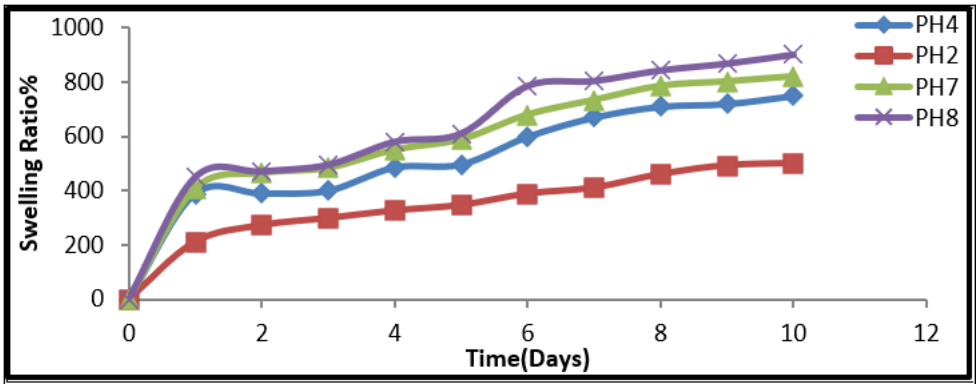

Figure(29): Swelling Ratio (Rs) For(PVP-Co-DMA-Co-(BADMA)) At Time Within Different Ph Range

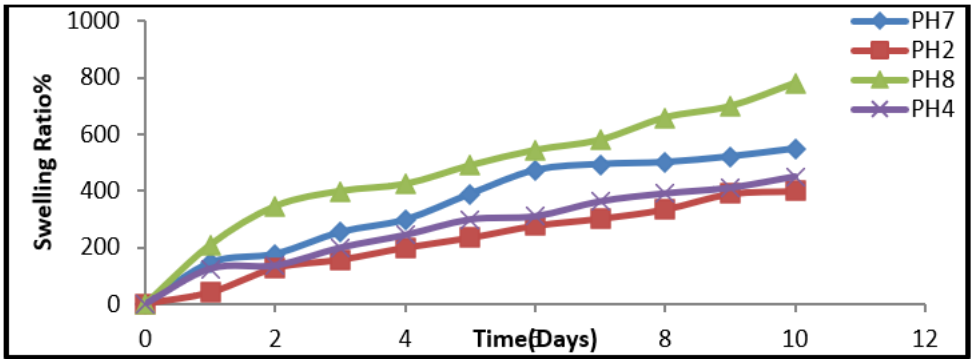

Figure(30): Swelling Ratio (Rs) For(MMA-Co-MA-Co-Cs) At Time Within Different Ph Range

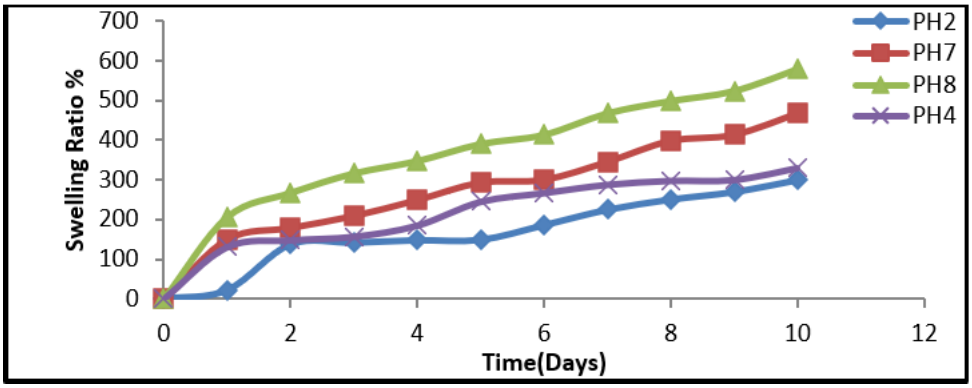

Figure(31): Swelling Ratio (Rs) For(EG-Co-MA-Co-PLA) At Time Within Different Ph Range

THE EFFECT OF PH ON ATENOLOL RELEASE

Figures (32-41) demonstrate the atenolol release rates from the (PLA-co-AA), (PLA-co-AA-co-DMA) **,** (PVP-co-DMA-co-(BADMA)) , (MMA-co-MA-co-Cs) and (EG-co-MA-co-PLA)hydrogels at pH 2, 4, 7, and 8 (19). Atenolol may release more quickly at pH values of 8 and 7, possibly as a result of the hydrogels' higher swelling ratio and the drug's weak H-bonding interaction with the polymer network. The drug-loaded device's macromolecular chains contain carboxylic groups of acrylic acid that are virtually entirely ionized. As a result, the polymeric chains go through a

significant amount of electrostatic relaxation. Finally, this causes the larger swelling ratio. While the decreased hydrogel swelling ratio at pHs 2 and 4 and the lack of induction of the chain relaxation process by unionized carboxylic groups may be responsible for the reduction in the amount of **Atenolol** released **[37].**

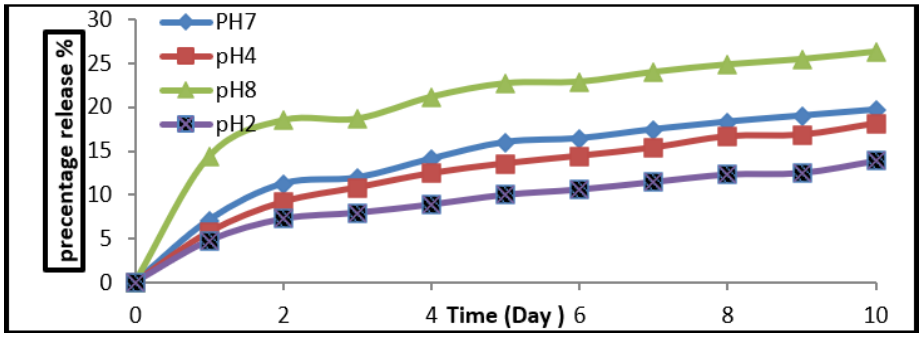

Figure 32: Percentage Drug Release From (PLA-Co-AA) At 37C°

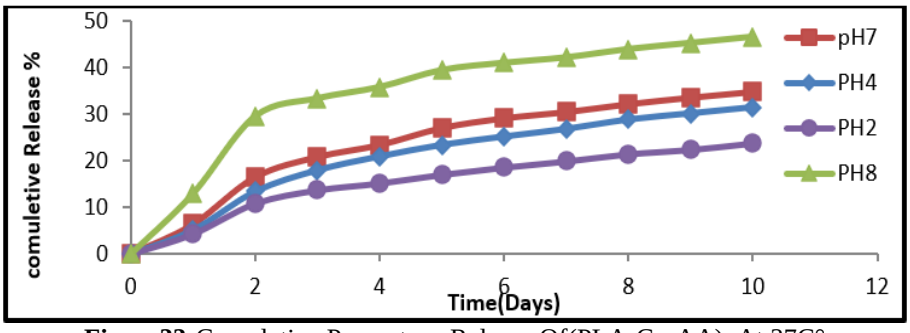

Figure33: Cumulative Percentage Release Of(PLA-Co-AA) At 37C°

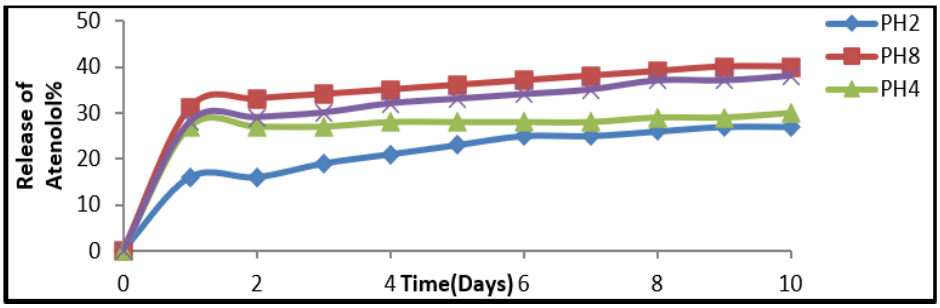

Figure 34: Percentage Drug Release From (PLA-Co-AA-Co-DMA) At 37C°

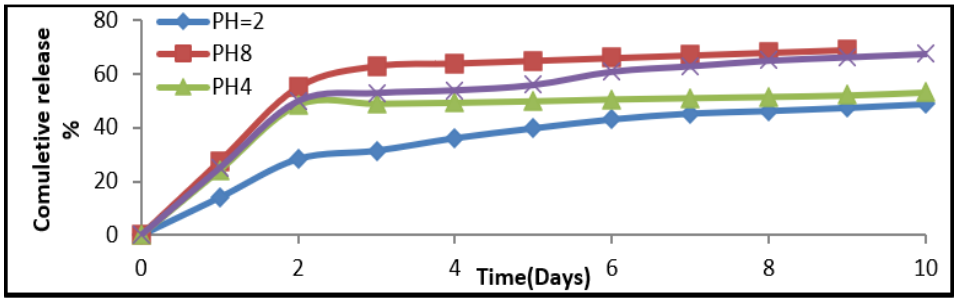

Figure 35 Shows The Cumulative Percentage Release Of (PLA-Co-AA-Co-DMA) At 37 °C.

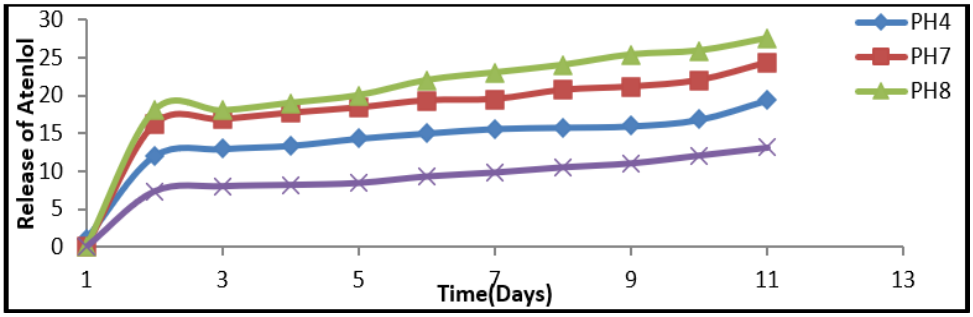

Figure 36: Percentage Drug Release From (PVP-Co-DMA-Co-(BADMA)) At 37C°

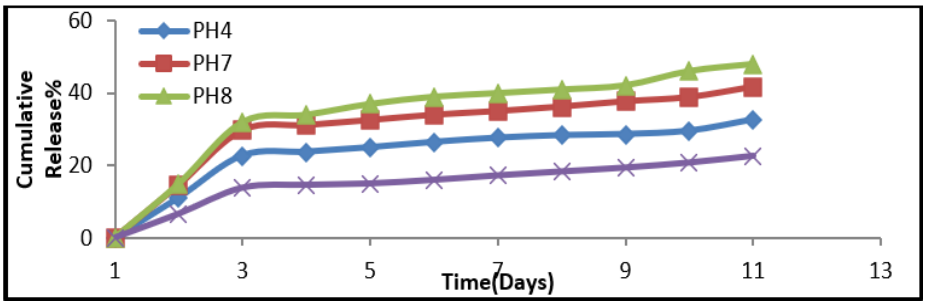

Figure 37: Shows The Cumulative Percentage Release Of (PVP-Co-DMA-Co-(BADMA)) At 37°C.

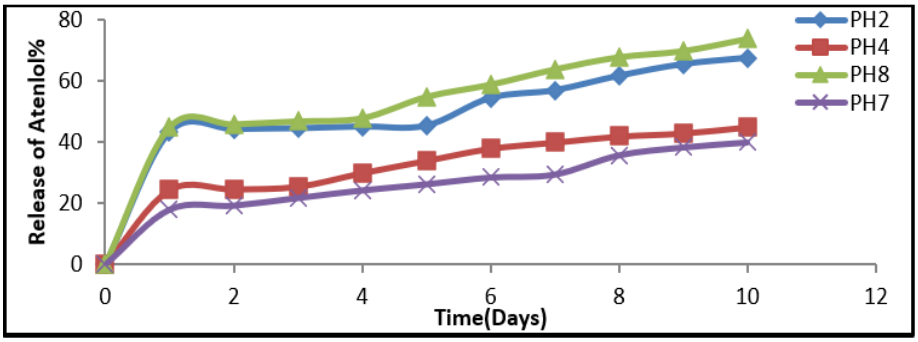

Figure 38: Percentage Drug Release From (MMA-Co-MA-Co-Cs) At 37C°.

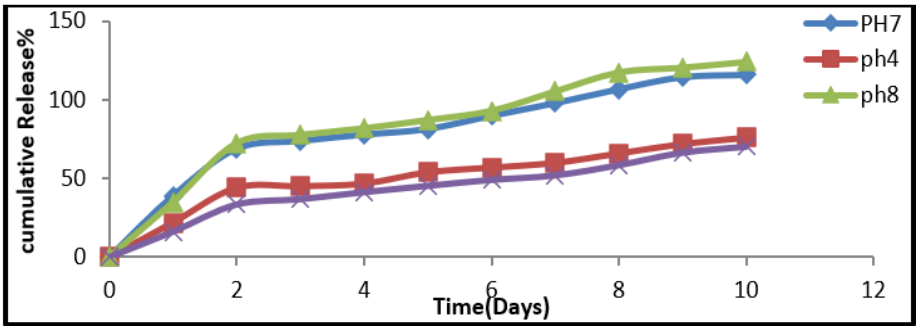

Figure 39: Shows The Cumulative Percentage Release Of (MMA-Co-MA-Co-Cs) At 37°C.

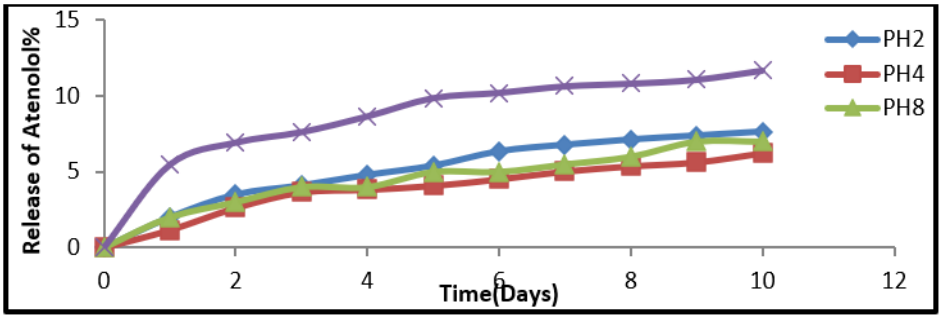

Figure 40: Percentage Drug Release From (EG-Co-MA-Co-PLA) At 37C°

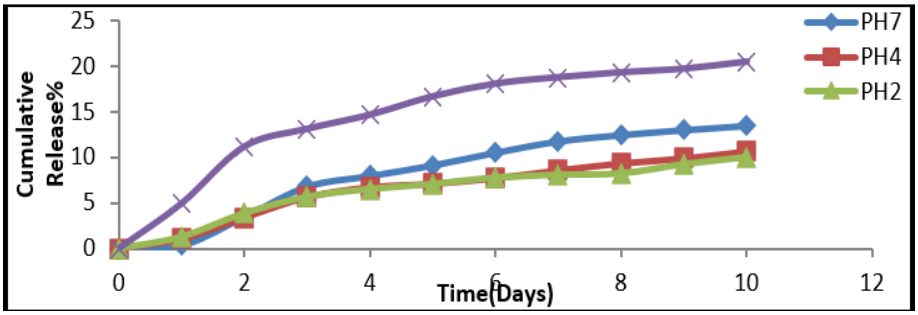

Figure 41: Shows The Cumulative Percentage Release Of (EG-Co-MA-Co-PLA) At 37°C.

TEMPERATURE EFFECTS ON ATENOLOL RELEASE

This study has also looked at how temperature affects the rate at which atenolol is released. As seen in figures (42) to (52), The release rate of **Atenolol** is found to be substantially lower at 37 ºC than it is at 39 ºC, that can be due to the decreased H-bonding caused by increasing the temperature. Which causes release of the drug to more speedily, as well as to an increase in the diffusivity and solubility of molecules loaded with atenolol within the superabsorbent. In the meantime, by increasing the diffusion pathways throughout the superabsorbent, the swelling ratio of the superabsorbent brought on by temperature changes possibly at least partially accountable for the rise in rate of atenolol release. Both of these two factors are thought to have influenced how quickly atenolol was released when the temperature increases **[37].**

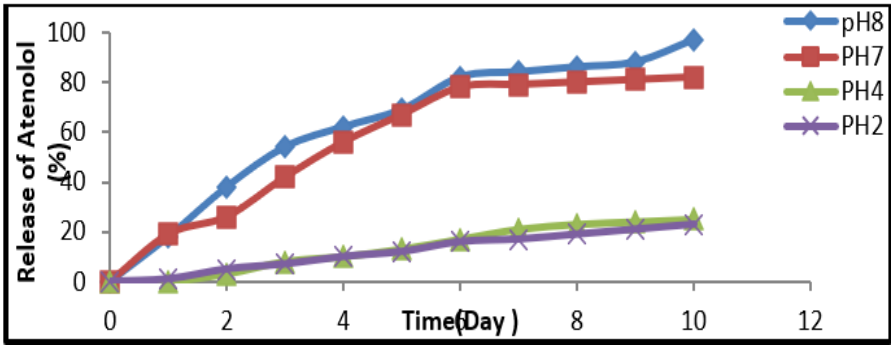

Figure 42: Percentage Drug Release From(PLA-Co-AA) At 39C°

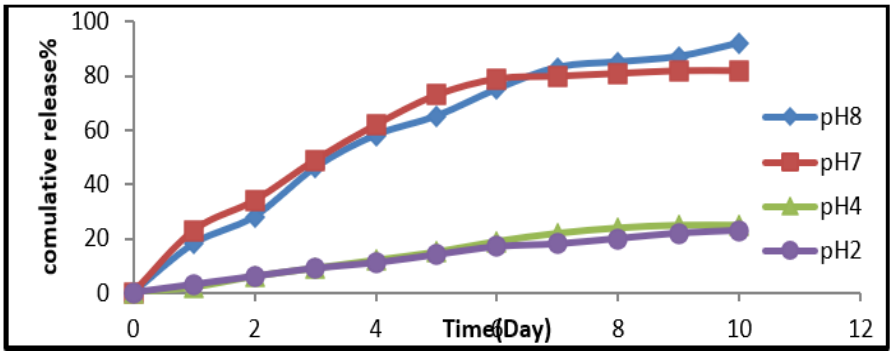

Figure43: Cumulative Percentage Release Of(PLA-Co-AA) At 39C°

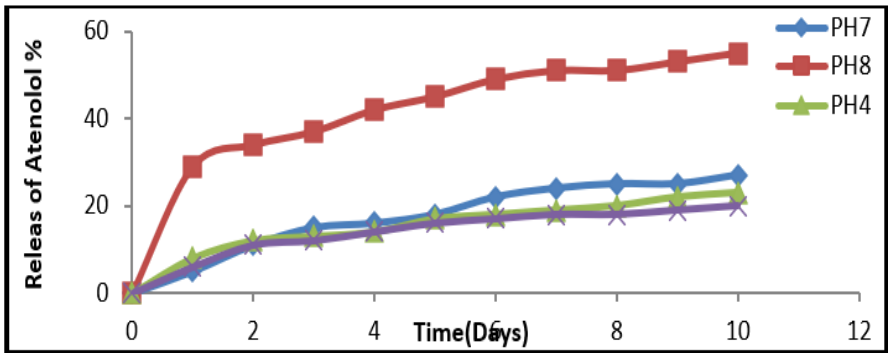

Figure 45: Percentage Drug Release From(PLA-Co-AA-Co-DMA) At 39C°

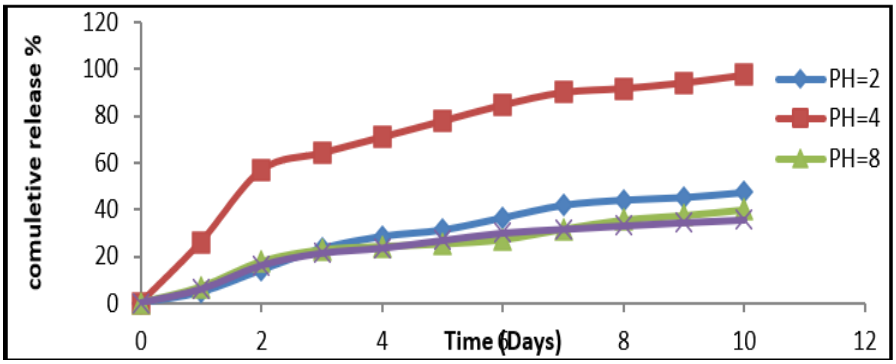

Figure46: Cumulative Percentage Release Of(PLA-Co-AA-Co-DMA) At 39C°

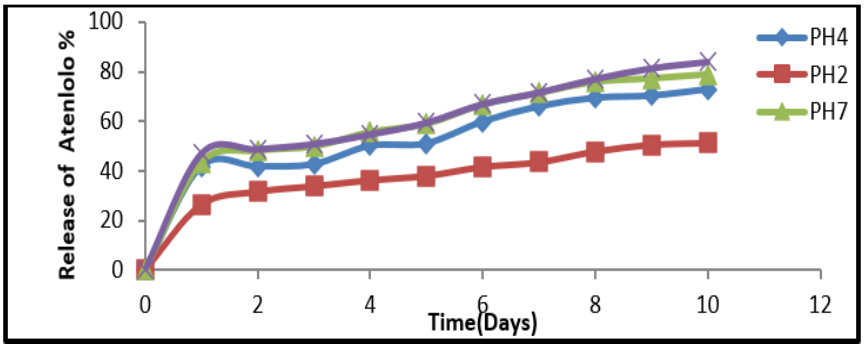

Figure 47: Percentage Drug Release From (PVP-Co-DMA-Co-(BADMA)) At 39C°.

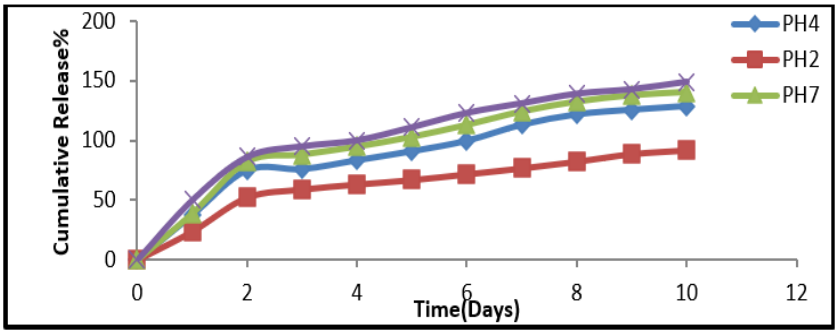

Figure 48: Shows The Cumulative Percentage Release Of (PVP-Co-DMA-Co-(BADMA)) At 39°C.

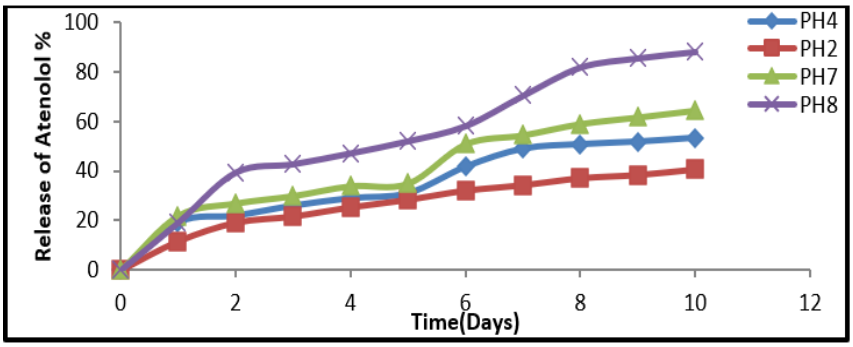

Figure49: Percentage Drug Release From (MMA-Co-MA-Co-Cs) At 39C°.

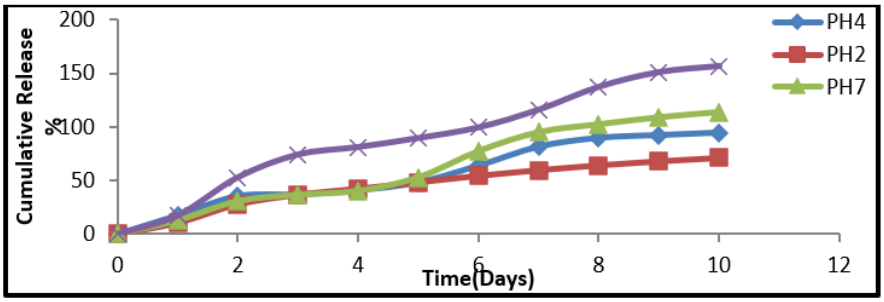

Figure 50: Shows The Cumulative Percentage Release Of (MMA-Co-MA-Co-Cs) At 37°C.

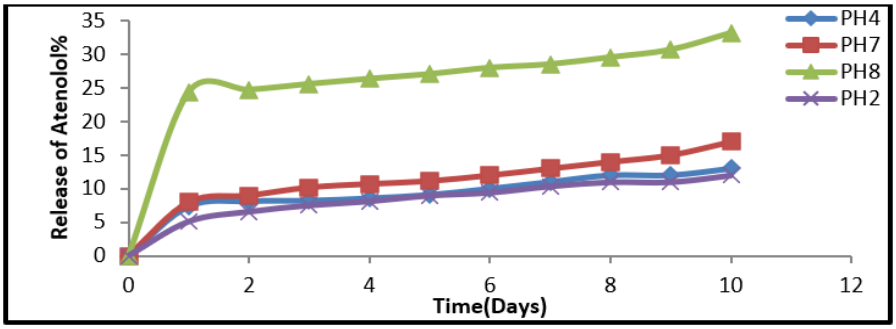

Figure51: percentage drug release from (EG-co-MA-co-PLA) at 39C°.

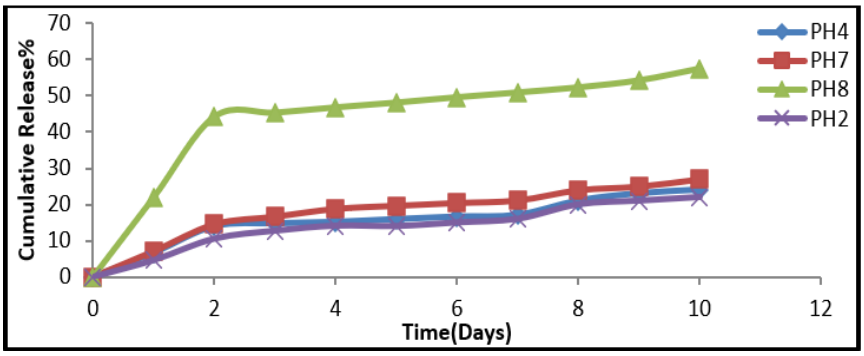

Figure 52: shows the cumulative percentage release of (EG-co-MA-co-PLA) at 39°C.

IN VIVO DRUG RELEASE STUDIES

Dexamethasone-salt is a common agent used to induce hypertension in laboratory animals **[38].** After 4 weeks of treatment, dexamethasone-salt markedly increased blood pressure compared to the saline group, as shown in the figures (53). Chronic administration of (Nanopolymer + Atenolol) reduced the increase in MSBP caused by dexamethasone, particularly polymer no.1 ((PLA-co-AA) + Atenolol), where the results showed that it has the best hypotensive effect, However, as shown in the figure(54), this hypotensive effect was not observed in normotensive rats

.

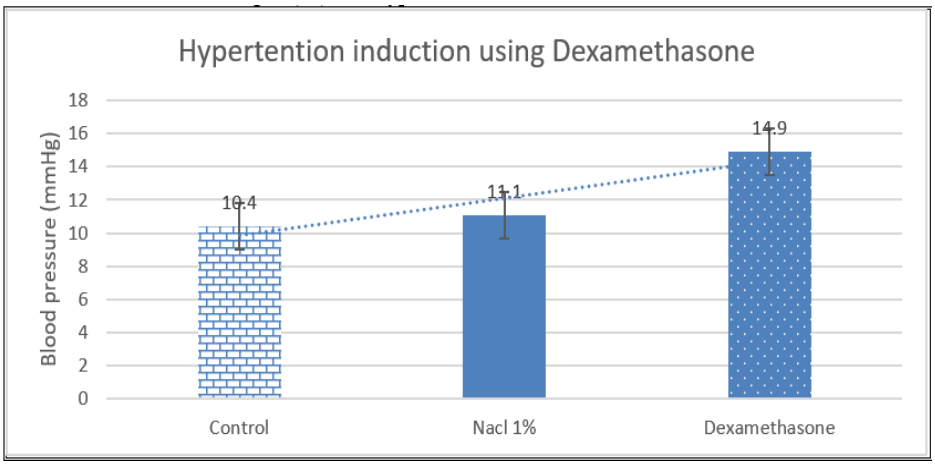

Figure 53: Dexamethasone-salt-induced hypertension after four weeks. Each value represents the mean SEM of six experiments, with *** P 0.05 vs normal saline-treated rats. ANOVA with a single way

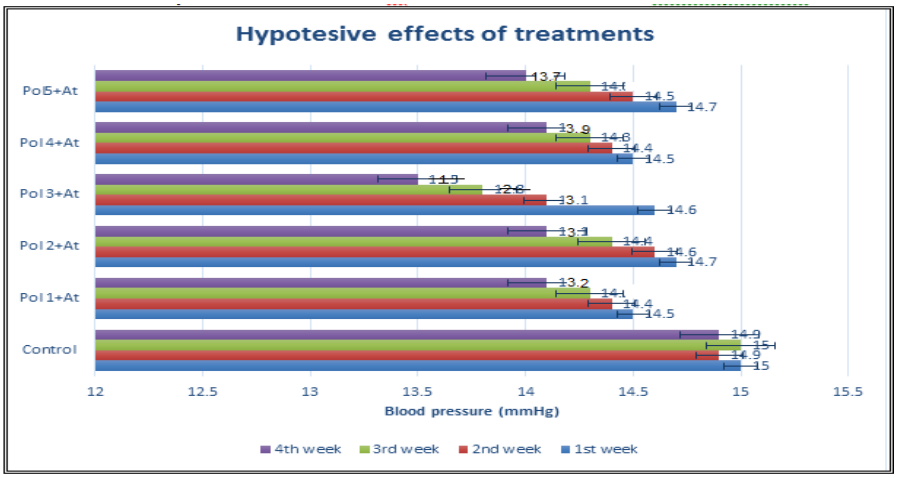

Figure 54: Mean systolic blood pressure (MSBP) in normotensive and hypertensive rats after four weeks of treatment with various doses of nanopolymer. Each number represents the mean SEM of six experiments.
***P 0.05 vs Dexamethasone-salt plus normal saline treated rats, one-way ANOVA

CONCLUSIONS

This work involved the synthesis and characterisation of nanocopolymers with different ratios of hydrophobic to hydrophilic monomers. This polymer, whose nanostructure measures between 40 and 88 nm. In order to create the molecularly imprinting polymer (MIP), the study applies chemical devices that use distinct monomers and a cross-linker to give the appropriate geometric shape. It also examines how each print may be made to be drug-ready. Atenolol was

used to study the modified hydrogel's drug-release ability. Where drug release experiments were conducted in four different media and were compared. The results show that increasing the pH increased the drug-release rate, providing us an appropriate method to control the release rate in different treatments. Its swelling behavior demonstrated greater temperature sensitivity in buffer solutions at various temperatures. The nature of the polymeric matrix influenced Atenolol release from hydrogels. All of these results indicate that nanocopolymers could be used as a temperature-responsive orally administered drug delivery system. The cumulative release showed low leakage at pH 2. The in vivo drug release has also been studied. A group of laboratory rats was divided into six groups, one group was a control group, and the five groups were administered with the nanopolymer powder under study loaded with atenolol drug after their pressure was raised by saline and dexamethasone group. The data confirmed that dexamethasone- salt significantly increased blood pressure compared to the saline group after 4 weeks of treatment. Chronic administration of (nanopolymer + atenolol) reduced the MSBP increase induced by dexamethasone, but this hypotensive effect was not observed in normal stress rats.

REFERENCES

1. Singh R, Lillard Jr JW. Nanoparticle-based targeted drug delivery. Experimental and Molecular Pathology 2009;86(3): 215-223.
2. Khan I, Saeed K, Khan I. Nanoparticles: Properties, applications and toxicities. Arabian Journal of Chemistry 2017.
3. Dash TK, Konkimalla VB. Poly-ϵ-caprolactone based formulations for drug delivery and tissue engineering: A review. Journal of Controlled Release 2012; 158(1): 15-33.
4. Szot CS, et al. Investigation of cancer cell behavior on nanofibrous scaffolds. Materials Science and Engineering: C 2011; 31(1): 37-42.
5. Hughes GA. Nanostructure-mediated drug delivery. Disease-a-Month 2005; 51(6): 342-361.
6. Faraji AH, Wipf P. Nanoparticles in cellular drug delivery. Bioorganic & medicinal chemistry 2009; 17(8):2950-2962.
7. Mansour HM, et al. Materials for pharmaceutical dosage forms: Molecular pharmaceutics and controlled release drug delivery aspects. International journal of molecular sciences 2010; 11(9): 3298-3322.
8. Qiu Y, Park K (2001) Environment-sensitive hydrogels for drug delivery. Adv Drug Deliv Rev 53:321
9. Maharaj I, Nairn JG, Campbell JB (1984) Simple rapid method for the preparation of enteric-coated microspheres. J Pharm Sci 73:39.
10. Hongsheng Guo · Xiwen He , Study of the binding characteristics of molecular imprinted polymer selective for cefalexin in aqueous media, Fresenius J Anal Chem, **368** :461–465, 2000.
11. Sonia Scorrano *, Lucia Mergola, Roberta Del Sole and Giuseppe Vasapollo, Synthesis of Molecularly Imprinted Polymers for Amino Acid Derivates by Using Different Functional Monomers, Int. J. Mol. Sci., **12**, 1735-1743, 2011.
12. Zhenkun Lin1, Wenjing Cheng1, Yanyan Li, Zhiren Liu, Xiangping Chen, Changjiang Huang A novel superparamagnetic surface molecularly imprinted nanoparticle adopting dummy template: An efficient solid-phase extraction adsorbent for bisphenol A, Analytica Chimica Acta **720** , 71– 76, 2012.
13. Komiyama M, Takeuchi T, Mukawa T, Asanuma H. Molecular imprinting from fundamentals to applications. Germany: Weinheim; 2003. p. 9–17.
14. Saifuddin N, Nur YA, Abdullah SF. Microwave enhanced synthesis of chitosan-graft polyacrylamide molecular imprinting polymer for selective removal of 17b-estradiol at trace concentration. Asian J Biochem.2011;6(1):38–54.
15. Cruickshank, R., Duguid, J. P., Marmion, B. P., Swain,R. H. A. and Churchill, L., Medical Microbiology, The Practice of Medical Microbiology, Edinburgh, New York, USA, (1975).
16. Tran, N. P. D. and Yang, M. C. (2019b) 'Synthesis and characterization of soft contact lens based on the combination of silicone nanoparticles with hydrophobic and hydrophilic monomers', Journal of Polymer Research. Journal of Polymer Research, 26(6), pp. 1–10. doi: 10.1007/s10965-019-1813-6.
17. Abou Taleb , M. F., Abdel-Aal, S. E., El-Kelesh, N. A.and Hegazy, E. A., Eur. Polym. J., 43 (2007) 468.
18. El˙zbieta C and Jacek N., Synthesis and Characterization Superabsorbent Polymers Made of Starch, Acrylic Acid, Acrylamide, Poly(Vinyl Alcohol), 2-Hydroxyethyl Methacrylate, 2-Acrylamido-2-methylpropane Sulfonic Acid). Int. J. Mol. Sci. 2021, 22, 4325
19. Lapiz-Bluhm MD, Soto-Pina AE, Hensler JG, Morilak DA. Chronic intermittent cold stress and serotonin depletion induce deficits of reversal learning in an attentional set-shifting test in rats. Psychopharmacology (Berl) 202: 329-341, 2009
20. Federica Tonolo, Laura Moretto, Stefania Ferro, Alessandra Folda ,Insight into antioxidant properties of milk-derived bioactive peptides in vitro and in a cellular model,Journal of Peptide Science 25(5), March 2019.
21. Mohsen-Imenshahidi, Bibi-Marjan-Razavi, Ayyoob-Faal , The Effect of Chronic Administration of Safranal on Systolic Blood Pressure in Rats. Iranian journal of pharmaceutical research , 14(2):585-90 .(2015)
22. Ashok Jadhav, Shuchita Tiwari, Paul Lee and Joseph Fomusi Ndisang,(The Heme Oxygenase System Selectively Enhances the Anti-Inflammatory Macrophage-M2 Phenotype, Reduces Pericardial Adiposity, and Ameliorated Cardiac Injury in Diabetic Cardiomyopathy in Zucker Diabetic Fatty Rats) Journal of Pharmacology and Experimental Therapeutics May 2013, 345 (2) 239-249;
23. Silverstien,R.M,Webster,F.X and Kiemle,D.J. (2005). Spectrometric identification of Organic compound 7th ed .Joun Wiley and Sons.
24. Pretsch,E., Buhlmann,P., and Baderscher,M. (2009).Structure determine of Organic compound 4th ed .springer-Verlag Berlin Heidelberg.
25. Pavia,L.D.,Lampman,L.G.,Kris,S.G.,andVyvyan,R.J.(2009).Introductionto Spectrophotometer 4 th.book cole general learning.
26. andrey tarasov." thermal analysis: methods, principles, applicason." lecture on thermal analysis 2012;26:16.2012.
27. K. B. Cantre, J. H. Martin and K. S. Ro," Application of Thermogravimetric Analysis for the Proximate Analysis of Livestock Wastes", Journal of ASTM International. 2009; 7(3)P:2-13.
28. R. v. adivarekar, s d dasarwar , n s khurana."synthesis of halogen free flame retardant and application polypropylene."indian journal of fibre &textile research vol 2012 ;38:pp:9-13.
29. D.a.babb , h.w.boone , d.w.smith and p.w.rudolf . "journal of applied polymer science" , 1998 ;69 : 2005-2012 .
30. Bernhard wunderlich . Thermal Analysis, text for an audio course. ATHAS, Advanced Thermal Analysis, Alaboratory for Research and Instruction 1981 .
31. Kim J. k. ,Cho G. B.: Modification of a crosslinked poly(acrylic acid) based new dehumidifying agent and its moisture absorbing characteristics. Macromolecular Research, **17** (7), 544-548, 2009.
32. Thakur,A.,Wanchoo,R.K.,and Singh,P. (2011). Hydrogels of Poly (acrylamide -co-acrylicacid):In-vitro Study on Release of Gentamicin Sulfate, Chem.Biochem. Eng. Q. 25 (4): 471–482.
33. HOLLY, F. J. (1981) 'Tear film physiology and contact lens wear. II. Contact lens-tear film interaction', Optometry and Vision Science. LWW, 58(4), pp. 331–341.
34. Sannino,A., Esposito, A., Nicolais, L., Del Nobile, M.A., Giovane, A., Balestrieri, C., Esposito, R., and Agresti, M. (2000).Cellulose-based hydrogels as body water retainers. J. Mater. Sci - Mater. Med., 11 (4):247-253.
35. Burdick, J.A., Ward, M., Liang, E., Young, M.J, and Langer, R. (2006). Stimulation of neurite outgrowth by neurotrophins delivered from degradable hydrogels. Biomaterials;27:452-9

36. (36)De, S. K. and Aluru, N.R., Mech. Mater., 36 (2004) 395.
37. Chen Y., Liang Y.:_A Sustained Release of Model Drug from a Novel Polyacrylic Acid- polyaluminium Chloride Superabsorbent._Iranian polymer journal,**19** (7),531-540,(2010).
38. G Tonolo , R Fraser, J M Connell, C J Kenyon . (Chronic low-dose infusions of dexamethasone in rats: effects on blood pressure, body weight and plasma atrial natriuretic peptide) J Hypertens. 1988;6(1):25-31.